Journal of Cleaner Production 442 (2024) 140827

Contents lists available at ScienceDirect

Journal of Cleaner Production

journal homepage: www.elsevier.com/locate/jclepro

Coupling input and output intensity to explore the sustainable agriculture intensification path in mainland China☆

Sijing Ye [a,b], Jilong Wang [b], Jiayi Jiang [b], Peichao Gao [a,b], Changqing Song [a,b,*]

[a] State Key Laboratory of Earth Surface Processes and Resource Ecology, Beijing Normal University, Beijing, 100875, China
[b] Faculty of Geographical Science, Beijing Normal University, Beijing, 100875, China

ARTICLE INFO

Handling Editor: Dr. Govindan Kannan

Keywords:
Sustainable intensification
Agriculture intensification
Suitability assessment
Coupling analysis
Arable land-use intensity
Land computing

ABSTRACT

Sustainable intensification (SI) of agriculture is widely regarded as an important way to alleviate the contradiction between the food gap and ecosystem health. Correlate input intensity and output intensity have been regarded as an important dimension in most estimation frameworks of SI. But in practice, this correlation is generally expressed in terms of efficiency metrics and calculated as the ratio of output intensity to input intensity, which cannot quantitatively explain the impact of input intensity on output intensity and provide a threshold value for estimating the suitability of SI. This study's goals are to propose an input—output coupled method to explain the impact of input intensity on output intensity and thereby estimate the suitability of provincial SI. Provincial annual input intensity and output intensity were estimated from an emergy-based perspective by taking China as a case study. The K-means algorithm was used to identify the structural pattern of arable land input intensity. A sliding window-based partial correlation index method was proposed and applied to reveal the interaction process between input intensity and output intensity. The results show that there are two main change paths in the pattern of input intensity: one path in the western irrigation regions and the other path in the eastern northeast China Plain and middle-lower Yangtze Plain. The former path can be expressed as a small increase in fertilizer and agro-machinery input intensity with a decrease in labour force input intensity. The latter path shows a larger increase in fertilizer and pesticide input intensity. For each type of input intensity except mulching film, its correlation to output intensity has experienced a similar coupling—decoupling—recoupling process in both plain provinces and mountainous or plateau provinces. According to Landau's theory of phase transition, the complex coupling of input and output undergoes a phase transition process from order to disorder and then to order, depicted by the sliding window-based partial correlation coefficient as the order parameter from a holistic perspective. The inflection points of coupling relation changes show that the phenomenon of fertilizer and pesticide overuse has steadily occupied most provinces in eastern China and is spreading westwards. Although the "zero growth action for fertilizers and pesticides" has made considerable achievements in reducing the input intensity of fertilizer and pesticides since 2015, the situation of superfluous fertilizer and pesticide input has not changed substantially. The input intensity of fertilizer and pesticides still needs to be further reduced. This study can contribute to the estimation method system of SI. The input—output coupled method is applicable for other spatial scales and regions (or countries) to estimate the suitability of SI.

1. Introduction

Currently, food security is confronted with great challenges (Rosegrant and Cline, 2003). Studies show that nearly 700 million people in the world still lack basic food supplies. Food production needs to be increased by 100 %–110 % to meet the expected demand due to population growth, changes in dietary structure and increased use of bioenergy (Tilman et al., 2011). This challenge is compounded by the fact that efforts to develop agriculture to meet food demand also need to balance ecosystem health and stability (Foley et al., 2011; Liu et al., 2023; Ye et al., 2023, 2024). For instance, excessive expansion of arable land has enormous impacts on habitats, biodiversity, carbon storage and soil conditions (Huang et al., 2021; Ren et al., 2022, 2023; Yin et al., 2022). Excessive fertilizer and pesticide inputs, irrigation water mining

☆ Sijing YE –), Associate Professor, specialized in arable land evaluation and protection. yesj@bnu.edu.cn
* Corresponding author. State Key Laboratory of Earth Surface Processes and Resource Ecology, Beijing Normal University, Beijing, 100875, China.
E-mail address: songcq@bnu.edu.cn (C. Song).

https://doi.org/10.1016/j.jclepro.2024.140827
Received 13 November 2023; Received in revised form 26 December 2023; Accepted 17 January 2024
Available online 30 January 2024
0959-6526/

and the promotion of heavy agricultural machinery have exacerbated climate change, biodiversity loss and degradation of land and freshwater (Zingg et al., 2018; Du et al., 2024; Ye et al., 2020a,b). Exploring sustainable agricultural development paths that reduce the harm of agriculture to the environment on the premise of meeting the growing food demand is related to the fate of all mankind.

Agricultural intensification is widely regarded as an important way to alleviate the contradiction between the food gap and ecosystem health, and its contribution to limiting arable land expansion and protecting biodiversity has been confirmed by multiple studies (Ewers et al., 2009; Hertel et al., 2014). The concept of "agricultural intensification" originated in the mid-19th century when Malthus (1798) explicitly addressed agricultural intensification in the context of population growth. In early studies, land-use intensity was rooted in land-rent theory (Von Thuenen, 1826) and the law of diminishing returns (Ricardo, 1815) and focused on enhancing crop yields through increased farming inputs (pesticides, fertilizers, seed, fuel or labour), tillage techniques and multicropping index. For instance, Brookfield (1993) defined agricultural intensification as "the substitution of inputs of capital, labour and skills for land, to gain more production from a given area, use it more frequently, and hence make possible a greater concentration of production". Subsequently, the impact of agricultural intensification on the environment has gradually received much attention, which reflects the transformation from intensification to sustainable intensification of agriculture.

The study of sustainable intensification (SI) can be traced back to the Agroecosystems Research Group's work report on sustainable intensification of tidal marshlands in Indonesia in 1983 (Wezel et al., 2015). Another early representative study is a collaborative project between researchers and farmers in sub-Saharan Africa in the 1990s (Pretty et al., 1996, 1997). The aim of the project is to build resilient agricultural systems that promote the synergistic development of crop output, livelihoods of the rural poor and environmental protection. Garnett et al. (2013) defined SI as "a process or production system that increases crop yield without additional land use and adverse environmental impacts". Lal (2019) consider SI an emerging agricultural model that maintains or improves environmental quality and increases agricultural production. Compared to agricultural intensification, SI focuses on the need to reduce the dependence of crop production on external inputs (e.g., fertilizer; pesticide), towards more 'restorative' production systems that stimulate nature-based solutions to supply nutrients and control pests (Pretty, 1997; Cassman and Grassini, 2020). Pretty and Bharucha (2014) summarized the transformation from intensification to SI from five aspects: a) breeding crops with high yield and insect resistance; b) making full use of agroecological processes such as nutrient cycling, biological control and biological nitrogen fixation; c) reducing toxic substance inputs; d) effectively using innovative farming techniques; and e) reducing negative externalities, such as limiting greenhouse gas emissions and preventing the spread of pests.

The estimation framework of SI has also gone beyond the original four dimensions of agricultural intensification (i.e., input intensity; output intensity; combined inputs and outputs; altered ecosystem services) (Erb, 2012; 2013; Kuemmerle et al., 2013; Ye et al., 2020a) towards a broader level by considering "productivity, economic sustainability, human wellbeing, environmental sustainability and social sustainability" (Petersen and Snapp, 2015; Smith et al., 2017; Reich et al., 2021). For instance, Smith et al. (2017) proposed a typical framework to track the development of SI for African smallholder farming systems, in which metrics from 6 dimensions, namely, productivity, economic sustainability, human well-being, environmental sustainability, social sustainability and gender equity, have been integrated. Mahon et al. (2018) collected 110 metrics of SI through semi-structured interviews with 32 stakeholders from the agri-food system in the UK. Based on the socioecosystem system (SES) framework, these metrics were classified into resource systems, resource units, management, resource users, interactions, outputs and the environment, but social and cultural factors were not considered (Mahon et al., 2018). Mouratiadou et al. (2021) presented a newly developed SI metrics framework (SIMeF) by integrating academic and policy indicator frameworks, expert opinions, and the Sustainable Development Goals to offer a holistic, generic, and policy-relevant dashboard for selecting SI metrics. The SIMeF consists of operating conditions, inputs, outputs, input–output relationships, environmental sustainability, economic sustainability and social sustainability. Other themes involve the impact of SI development on arable land productive capacity, soil health and ecological health (Li et al., 2019; Wang et al., 2022a; Ye et al., 2022a, 2022b); specific SI practices to increase crop yield at low environmental cost (Gregory et al., 2002; Chen et al., 2011; Zhang et al., 2017; Mckay et al., 2019); the "land sparing" vs. "land sharing" debate (Green et al., 2005; Phalan et al., 2016; Desquilbet et al., 2017); and simulation studies of optimizing crop structure and spatial distribution to feed the earth with small negative externalities (Foley et al., 2005; Mehrabi et al., 2018; Folberth et al., 2020).

The above studies make an important contribution to developing the theory and implementation plan of sustainable intensification. Estimating the regional suitability of SI at national and global scales provides guidance for adjusting land use intensity and structure to better cope with the conflict between food demand, economic development and ecological protection. Correlate input intensity and output intensity have been regarded as important dimensions in most SI estimation frameworks (Herzog et al., 2006; Pretty et al., 2018; Cassman and Grassini, 2020). However, in practice, this correlation is expressed in terms of efficiency metrics, which are generally calculated as the ratio of output intensity to input intensity (e.g., yield per unit input of energy, water and nutrients; nitrogen utilization rate). With this approach, the complex nonlinear relationship between input and output has been ignored (Zhang et al., 2015; Smith et al., 2017; Mouratiadou et al., 2021). For instance, arable land under extensive management may achieve high "efficiency" because of its extremely low input. Vanlauwe et al. (2010, 2014) try to solve this issue by controlled trials and calculate the difference (abbr. D) between maize yield in the treatment with fertilizer application and that in no-input control inputs; then, the SI of each trial point i is estimated as the ratio of D_i to D_{max}. Another computational idea of efficiency is the ratio between actual yield (observed yields) and a maximum yield that is attained under similar climate and soil conditions and optimal management measures (Neumann et al., 2010; Dietrich et al., 2012; Yin et al., 2020). Whereas, it still confuses us how to quantitatively describe the impact of input intensity on output intensity and thereby estimate the suitability of SI. By combining sliding window and partial correlation coefficient, calculating the coupling relationship between input intensity and output intensity in different numerical ranges, the influence process of input intensity on output intensity can be expressed.

The estimation of agricultural SI involves many dimensions including operating conditions, inputs, outputs, input–output relationships, environmental sustainability, economic sustainability and social sustainability (Mouratiadou et al., 2021). The theme of this study focuses on one dimension: input–output relationships. The authors estimate provincial annual input intensity and output intensity from an emergy-based perspective by taking China as a study case. The K-means algorithm was used to identify the structural pattern of the provincial annual arable land input intensity. Then, a sliding window-based partial correlation index method (also called the "input—output coupled method") was proposed and applied to reveal the coupling—decoupling—recoupling process between input intensity and output intensity. According to this process, the early warning threshold and critical warning threshold of fertilizer (or pesticide) input intensity have been designed to estimate the suitability of provincial SI. Furthermore, the impact degree of input factors on output intensity was estimated by a random forest model, and the SI status of China was discussed from a global perspective. This study can contribute to the estimation method system of SI. In particular, the input—output coupled method is applicable to other spatial scales and regions for understanding the relationship between input and output.

2. Material and methods

2.1. Data

In this study, 3 kinds of datasets are used to estimate arable land use intensity based on emergy synthesis. First, the annual provincial crop production dataset, farming input dataset and crop sown area dataset of China during 1998–2019 were used to estimate output intensity and input intensity. These datasets are extracted from the China rural statistical yearbook (1999–2020). The crop production dataset and crop sown area dataset cover annual provincial production (unit: metric ton) and sown area (unit: ha.) of all main crop types in mainland China, including rice and paddy, wheat, maize, pulses, roots and tubers, oil of vegetal origin, sugar crops, and vegetables. The farming input dataset contains annual provincial input quantity of yield-enhancing substances (i.e., pesticide; chemical fertilizer; mulching film), labour force (i.e., agricultural registered population) and agro-machinery input (e.g., total power of agricultural machinery). Second, global national agricultural output and input datasets are extracted from FAOSTAT between 1995, 2000, 2005, 2010, 2015 and 2019 to estimate the global national arable land output and input intensity. The global national agricultural output dataset covers production quantity (unit: metric ton) and sown area (unit: ha.) of all main crop types in the world. The Global national agricultural input dataset contains annual national input quantities of pesticides and chemical fertilizers. Third, the nutritive conversion coefficient dataset indicates Calorie absorbed by the human body per ton of multiple crop types (unit: kilojoules per metric ton) (*see Appendix A.1 for detailed coefficient data*). The nutritive conversion coefficient dataset has been used to convert the production quantity of different types of crops to unified and comparable energy units. The solar emergy conversion coefficient is quoted from Lu et al. (2005) and Yao et al. (2014b). It is used to unify the dimension of different farming input factors (*see* Appendix A.2 *for detailed coefficient data*). Table 1 shows detailed dataset information.

2.2. Calculation of the provincial annual arable land input intensity

Provincial annual arable land total input intensity ($ALUI_{in\_total}$, unit: sej/ha.) is calculated as the summation of fertilizer input intensity ($ALUI_{in\_fer}$), pesticide input intensity ($ALUI_{in\_pes}$), mulching film input intensity ($ALUI_{in\_mf}$), agro-machinery input intensity ($ALUI_{in\_am}$) and labour force input intensity ($ALUI_{in\_lab}$), as shown in Eq. (1) shows. SET is solar emergy conversion coefficient of specific element *(see* Appendix A.2 *for detailed information)*: SET_{FN} is solar emergy conversion coefficient of nitrogen fertilizer (unit: sej/ton); SET_{FP} is solar emergy conversion coefficient of phosphate fertilizer (unit: sej/ton); SET_{FK} is solar emergy conversion coefficient of potassic fertilizer (unit: sej/ton); SET_{FC} is solar emergy conversion coefficient of compound fertilizer (unit: sej/ton); SET_{lab} is solar emergy conversion coefficient of labour force (unit: sej/per capita); SET_{pes} is solar emergy conversion coefficient of pesticide (unit: sej/ton); SET_{mf} is solar emergy conversion coefficient of mulching film (unit: sej/ton); SET_{am} is solar emergy conversion coefficient of agricultural machinery (unit: sej/kwh). Q is the provincial annual input quantity of a specific element: Q_{FN} is the quantity of nitrogen chemical fertilizer input (unit: metric ton); Q_{FP} is the quantity of phosphate chemical fertilizer input (unit: metric ton); Q_{FK} is the quantity of potassic chemical fertilizer input (unit: metric ton); Q_{FC} is the quantity of compound chemical fertilizer input (unit: metric ton); Q_{pes} is the quantity of pesticide input (unit: metric ton); Q_{mf} is the quantity of mulching film input (unit: metric ton); and Q_{am} is the total power of agricultural machinery (unit: kwh). Q_{lab} is the quantity of labour force input (unit: capita). S_i indicates the provincial annual sown area of crop i. n is the number of crop types.

$$ALUI_{in\_total} = ALUI_{in\_fer} + ALUI_{in\_pes} + ALUI_{in\_mf} + ALUI_{in\_am} + ALUI_{in\_lab} \quad \text{Eq. (1)}$$

$$ALUI_{in\_fer} = \frac{(Q_{FN} * SET_{FN}) + (Q_{FP} * SET_{FP}) + (Q_{FK} * SET_{FK}) + (Q_{FC} * SET_{FC})}{\sum_{i=1}^{n} S_i} \quad \text{Eq. (2)}$$

Table 1
Detailed dataset information related to the estimation of arable land use intensity.

Dataset	Definition	Data source	Applications
Annual provincial crop production of China	Annual production of multiple types of crop *i* (unit: metric ton), including rice & paddy; wheat; maize; pulses; roots and tubers; oil of vegetal origin; sugar crops; vegetables.	China rural statistical yearbook (1999–2020)	(Li et al., 2001; Yao et al., 2014a, 2014b)
Annual provincial farming inputs of China	Annual farming input quantity of pesticides (unit: metric ton); chemical fertilizer (unit: metric ton); mulching film (unit: metric ton); agricultural diesel (unit: metric ton); labour force (unit: metric capita).	China rural statistical yearbook (1999–2020)	(Yao et al., 2014a; Yin et al., 2018, 2020; Xie et al., 2020)
Annual provincial crop sown area of China	Annual sown area of crop *i* (unit: ha.), including rice & paddy; wheat; maize; pulses; roots and tubers; oil of vegetal origin; sugar crops; vegetables.	China rural statistical yearbook (1999–2020)	(Ye et al., 2019, 2020a, 2022b)
Global national agricultural output	Annual production quantity (unit: metric ton) and area harvested (unit: ha.) of multiple types of crop *i*, including rice & paddy; wheat; maize; beans dry; potatoes; sweet potatoes; Cassava.	FAOSTAT. (https://www.fao.org/faostat/en/#data/QCL) (1995, 2000, 2005, 2010, 2015, 2019)	(Shriar, 2000; Smith, 2013)
Global national agricultural input	Annual agricultural use quantity of pesticides (unit: metric ton); chemical fertilizer (unit: metric ton).	FAOSTAT. (https://www.fao.org/faostat/en/#data/RP) & (https://www.fao.org/faostat/en/#data/RFN) (1995, 2000, 2005, 2010, 2015, 2019)	(Smith, 2013)
Nutritive conversion coefficient	Calories absorbed by human body for per ton of crop *i* (unit: kilojoules per metric ton), including rice & paddy; wheat; maize; pulses; roots and tubers; oil of vegetal origin; sugar crops; vegetables.	FAOSTAT. (http://www.fao.org/food-agriculture-statistics/statistical-domains/crop-livestock-and-food/methodology/en/)	Tilman et al. (2011)
Solar Emergy conversion coefficient	Coefficient for converting pesticide input; chemical fertilizer input; mulching film input; labour force input and agricultural diesel input to solar emergy equivalents (unit: sej/t).	(Lu et al., 2005; Yao et al., 2014b)	(Lu et al., 2005; Xie et al., 2012; Yao et al., 2014b; Yin et al., 2020)

$$ALUI_{in\_pes} = \frac{Q_{pes} \times SET_{pes}}{\sum_{i=1}^{n} S_i} \quad \text{Eq. (3)}$$

$$ALUI_{in\_mf} = \frac{Q_{mf} \times SET_{mf}}{\sum_{i=1}^{n} S_i} \quad \text{Eq. (4)}$$

$$ALUI_{in\_am} = \frac{Q_{ad} \times SET_{ad}}{\sum_{i=1}^{n} S_i} \quad \text{Eq. (5)}$$

$$ALUI_{in\_lab} = \frac{Q_{lab} \times SET_{lab}}{\sum_{i=1}^{n} S_i} \quad \text{Eq. (6)}$$

The global national annual fertilizer input intensity and pesticide input intensity are also calculated by Eq. (2) and Eq. (3), respectively. The difference is that Q_{FN}, Q_{FP}, Q_{FK}, Q_{FC}, and Q_{pes} should be replaced with the national input quantity of the corresponding elements; S_i should be replaced with the national annual total area of crop i. For each type of input intensity in a specific province (or country), the change rates between adjacent years were calculated, and three standard deviation methods were used to identify outliers with abnormal changes. These outliers are mainly due to statistical error and have been replaced by the average value of samples from their surrounding years. This method has also been used to identify and modify outliers in arable land output intensity in Section 2.3.

2.3. Calculating the provincial annual arable land output intensity

The provincial annual arable land output intensity $ALUI_{out}$ is calculated by Eq. (7). For a specific year and province, Y_i is the total production of crop i (unit: metric ton). NCC_i is the nutritive conversion coefficient of crop i (unit: kJ/ha) *(see* Appendix A.1 *for detailed information)*. S_i presents the provincial annual sown area of crop i (unit: ha.). n is the number of crop types. The global national annual output intensity is also calculated by Eq. (7). The difference is that Y_i, NCC_i, S_i should be replaced with the national quantity of corresponding elements.

$$ALUI_{out} = \frac{\sum_{i=1}^{n} (Y_i \times NCC_i)}{\sum_{i=1}^{n} S_i} \quad \text{Eq. (7)}$$

2.4. Calculation of the partial correlation index based on the sliding window

Multiple types of input intensity comprehensively influence output intensity. For each type of input intensity, its correlation with output intensity has been presented by the partial correlation coefficient to reduce the influence of other types. The partial correlation coefficient can be calculated by Eq. (8). $\rho_{XY|Z}$ is the partial correlation coefficient of the control variables Z for variables X and Y, and $\hat{\epsilon}, \hat{\delta}$ are the residuals of the multiple linear regression established between X, Y and Z, respectively. $\text{cov}(\hat{\epsilon}, \hat{\delta})$ is the correlation coefficient of $\hat{\epsilon}, \hat{\delta}$; $\text{cov}(\hat{\epsilon}, \hat{\delta})$ is the covariance of $\hat{\epsilon}, \hat{\delta}$; and $var(\hat{\epsilon})$ *and* $var(\hat{\delta})$ are the variances of $\hat{\epsilon}, \hat{\delta}$. The residuals $\hat{\epsilon}, \hat{\delta}$ eliminate the linear correlation between X, Y and Z. Thus, calculating the correlation coefficient between $\hat{\epsilon}, \hat{\delta}$ gives its partial correlation coefficient.

$$\rho_{XY|Z} = \text{cor}(\hat{\epsilon}, \hat{\delta}) = \frac{\text{cov}(\hat{\epsilon}, \hat{\delta})}{\sqrt{var(\hat{\epsilon})}\sqrt{var(\hat{\delta})}} \quad \text{Eq. (8)}$$

According to land rent theory, input intensity may have different effects on output intensity in its different value ranges. A sliding window was used to calculate the partial correlation coefficient in multiple value ranges. Taking fertilizer input intensity as an example, the detailed implementation process is as follows (Fig. 1).

◇ Step 1, normalize the fertilizer input intensity value of all samples to the range of 0–100 and arrange them in ascending order.
◇Step 2, set the size and step width of the initial sliding window as ws and l. The corresponding initial value range is [0, ws].
◇Step 3, extract samples whose normalized fertilizer input intensity values belong to the initial value range (i.e., [0, ws]). The partial correlation coefficient between the normalized fertilizer input intensity and output intensity was calculated. The result is expressed as a point in the Cartesian coordinate system, with the partial correlation coefficient set as the y-coordinate and the average value of the extracted samples' normalized fertilizer input intensity as the x-coordinate.
◇Step 4, slide the window by a step width of l, and then the value range turns to [l, $ws + l$]. Extract samples and calculate the partial correlation coefficient by following the calculation process in step 3.
◇Step 5, repeat the calculation process in Step 4 until the upper bound of the value range is greater than or equal to 100. Fig. 1 shows the difference in the partial correlation coefficient and its significance in sliding windows with different value ranges.

3. Result

3.1. National arable land use intensity in China

As shown in Fig. 2(a), the output intensity of staple food grains (including rice; wheat; corn; beans; potato) and oil crops (oilseed and hemp) both show steady increases from 1998 to 2019. The former increases from 5.81e+07 to 7.64e+07, and the latter increases from 6.63e+07 to 10.00e+07 (unit: kJ/ha.). Before 2015, the total input intensity increases synergistically with output intensity, increasing from 112.87e+13 to 147.81e+13 (unit: sej/ha.). Then, the total input intensity decouples from the output intensity and decreases to 128.73e+13 in the subsequent five years. The decline in fertilizer input intensity after 2015 is the primary reason for the decline in total input intensity because it accounts for a large proportion (88.28 %–90.75 %) of total input intensity (Fig. 2(b)). The pesticide input intensity showed a similar changing pattern of increasing and then declining and dropped to nearly the initial degree in 1998 from 2015 to 2019 (Fig. 2(c)). This demonstrates that "zero growth action for fertilizers and pesticides" by the Ministry of Agriculture and Rural Affairs of PRC since 2015 has made considerable achievements. The proportion of fertilizer input intensity is in continuous decline with fluctuations, although its value obviously increases before 2015. This is because the Agro-Machinery has experienced dramatic growth from 5.52e+13 to 11.43e+13 (Fig. 2(d)). As shown in Fig. 2(e), there has been a continuous reduction in labour force input intensity since 2003. The white pollution caused by nondegradable mulching film is becoming more serious as the input intensity of mulching film increased sharply from 1998 to 2014 and then remained stable in subsequent years (Fig. 2(f)).

3.2. Provincial arable land input and output intensity

Wald's method has been used to divide the annual total arable land input intensity of multiple provinces into three stages, namely, 1998–2003 (stage 1); 2004–2011 (stage 2); and 2012–2019 (stage 3) (see *Appendix B.1* for the details of the stage division). On that basis, spatial and temporal differences in provincial total arable land input intensity are listed in Fig. 3(a). Fig. 3(b) shows the spatial and temporal differences in three types of input intensity (i.e., yield-enhancing physical inputs; labour inputs and agricultural machinery inputs) at the provincial level (see *Appendix B.2* for supplementary maps). Provinces in

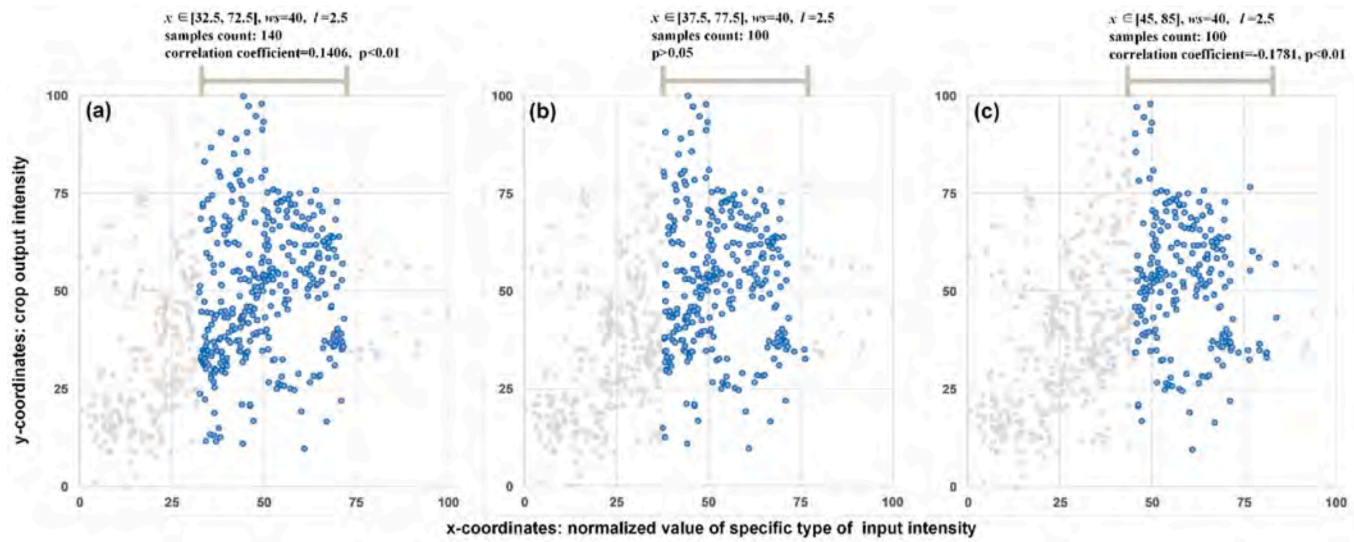

Fig. 1. Implementation process of calculating the partial correlation index based on a sliding window. The x-coordinate is the normalized value of a specific type of input intensity (e.g., fertilizer input intensity). The y-coordinate is the normalized value of the crop output intensity. (a)–(c) show calculation of the partial correlation coefficient in sliding windows with different value ranges.

the Huang-Huai-Hai Plain and Southern China show the highest input intensity with obvious clustering features. The former shows a combination of high physical inputs and high agro-machinery inputs with low dependency on labour inputs, while the latter is highly dependent on physical and labour inputs with moderate level agro-machinery inputs. The physical inputs of provinces with large plain areas are obviously higher than those of mountainous provinces, except for Heilongjiang Province (see *Appendix C.1* for supplementary classification of plains provinces and mountainous provinces). For nearly all provinces, the labour input intensity decreases, and the agro-machinery input intensity increases. This demonstrates that the spread of agricultural machinery reduced the dependence of farming on labour inputs. Major grain-producing provinces generally present higher input intensity than other provinces. Heilongjiang, Inner Mongolia, Anhui, Jiangxi, Hunan and Sichuan have high potential to enhance input intensity. Heilongjiang, Qinghai and Guizhou show the lowest input intensity. The annual input intensity of Xinjiang, Shaanxi, Zhejiang and Guangxi has experienced a substantial increase. The high total input intensity in Beijing and Tibet is because of the dramatic reduction in harvested area. This leads to an extremely low physical input intensity and excessive agricultural machinery power in Tibet.

Fig. 4(a) and (b) show the provincial annual output intensity of staple food grains and oil crops, respectively. The high output intensity of staple food grains shows the characteristics of aggregation in the great plains of China, namely, the Northeast China Plain, Huang-Huai-Hai Plain and Middle-lower Yangtze Plain. Inner Mongolia, Ningxia, Hebei, Henan, Anhui, Jiangxi, and Hubei experienced a substantial increase in the output intensity of staple food grains in stage 1 and stage 2. In stage 3, the output intensity of staple food grains tends to be stable for most provinces. Provinces in the Sichuan Basin and surrounding areas, the Yunan-Guizhou Plateau and southern China show continuous low output intensity of staple food grains. In Tibet, large amounts of low-quality arable land have been transformed for ecological conservation since the 1990s, which has led to a high-level output intensity of staple food grains. The increase in the provincial annual output intensity of oil crops indicates a gradually generalized phenomenon of “nonfood”. The development of oil crop output intensity in plain regions tends to occur earlier than that in mountainous areas. Southern China shows a high-level output intensity of oil crops. This indicates an SI level of agriculture inconsistent with that indicated by the output intensity of staple food grains.

Combining input intensity (Fig. 3) and output intensity (Fig. 4) shows that there are disadvantages to indicating arable land use intensity from a single-dimensional perspective. First, improving the input intensity level or structure is not always applicable to indicate the agricultural development level and benefits. For instance, Heilongjiang Province achieves high output intensity of staple food grains, although its intensity of physical inputs, labour inputs and agricultural machinery inputs is low. It also demonstrates that arable land quality has an important influence on the relationship between input and output intensity. Second, the efficiency of output intensity is constrained by input intensity. For instance, the high input intensity in Southern China does not lead to high output intensity of staple food grains. From the overall point of view, the high output intensity of staple food grains shows high dependence on input intensity.

3.3. Identify the pattern of provincial arable land input intensity

The K-means algorithm was used to identify the pattern of provincial annual arable land input intensity. Each input sample consists of the provincial annual normalized input intensity of fertilizer, pesticides, agro-machinery, labour force and mulching film for one specific year. The triple standard deviation method was used to filter out the outlier value of each input intensity element. During the process of applying the K-means algorithm, the number of categories needs to be manually set in advance. To explore the appropriate number of categories, we have designed 7 classification schemes, corresponding to 2 categories, 3 categories, 4 categories, 5 categories, 6 categories, 7 categories and 8 categories respectively. The sum of squares due to error (abbr. SSE) index, silhouette score (abbr. SC) index and Calinski-Harabaz (abbr. CH) index have been used to determine the appropriate number of categories (Fig. 5) (*see detailed computing method in* Appendix B.3, B.4). The results show that the pattern of provincial annual arable land input intensity fits best into five categories. This is because the scheme of “5 categories” shows the maximum descent gradient of the SSE index, a better SC index than the scheme of “4/6/7 categories” and a better CH than the scheme of “6/7/8 categories”.

The structural pattern of the provincial annual arable land input intensity was divided into 5 classes. The characteristics of each class are portrayed in Fig. 6(a). Class A presents an input structure with relatively high mulching film, middle level fertilizer and agro-machinery, low level pesticides and labour force. Class B indicates an input structure

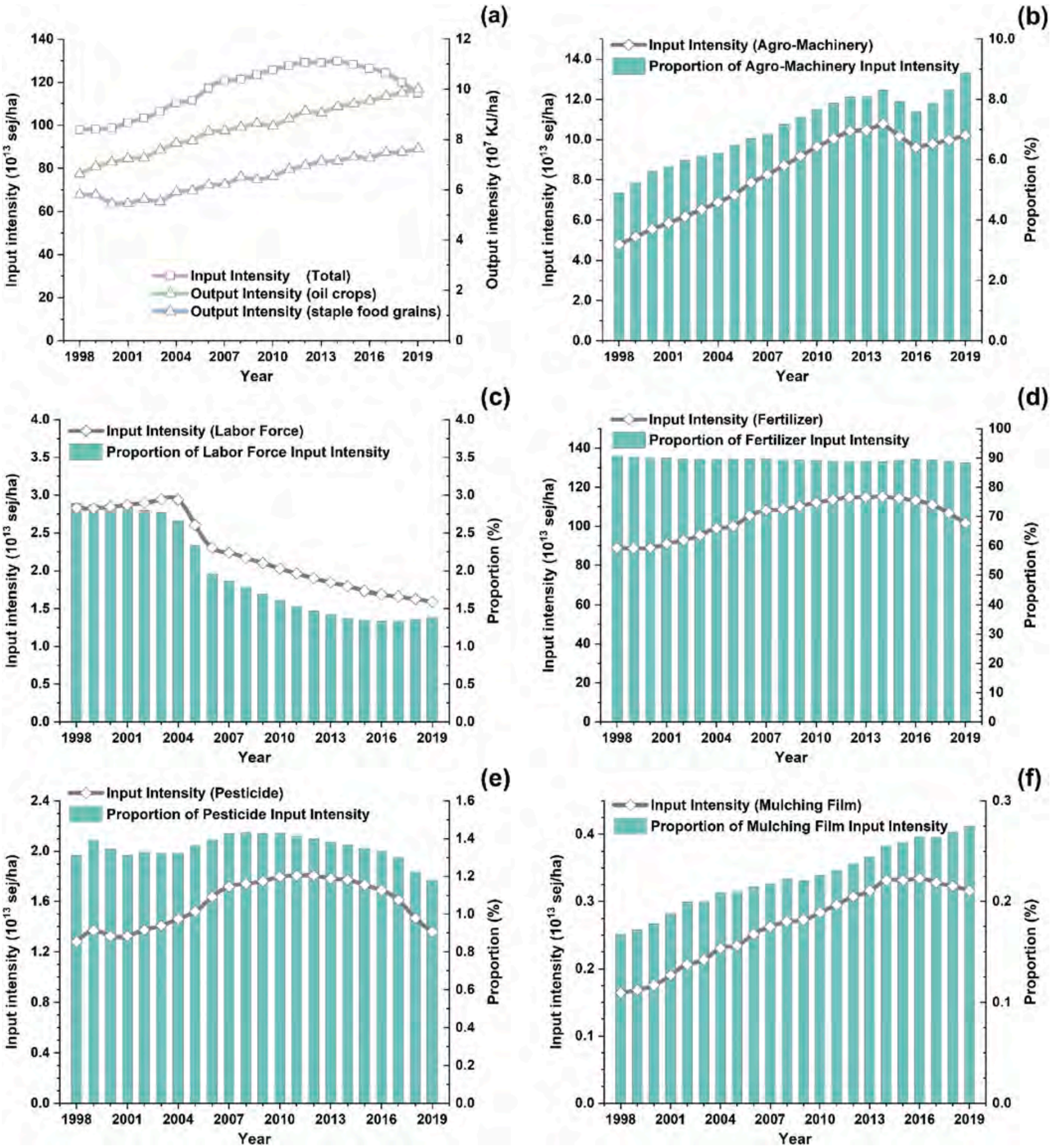

Fig. 2. Overall arable land use intensity in China from 1998 to 2019. (a) Annual total input intensity (unit: sej/ha.), output intensity (unit: kJ/ha.) of staple food grains (including rice; wheat; corn; beans; potato) and oil crops (oilseed; hemp). (b)–(f) show multiple components (i.e., (b) fertilizer; (c) pesticides; (d) agro-machinery; (e) labour force; (f) mulching film) of input intensity and their proportion (%) to total input intensity from the perspective of emergy. Hong Kong, Macau and Taiwan are not participating in the calculation due to lack of data.

that relies heavily on the labour force with low-level yield-enhancing physical inputs and agricultural machinery inputs. Class C presents input structures that seem appropriate for large-scale agricultural operations: high fertilizer inputs with high agricultural mechanization conditions. Class D and E show similar high fertilizer input intensity to Class C. The difference is that Class D highly depends on the labour force and pesticides with middle-level agricultural machinery inputs; Class E corresponds to middle-level pesticide and agricultural machinery inputs.

Fig. 6(b) shows the spatial-temporal variation in the structure pattern of arable land input intensity. In stage 1 (1998–2003), many provinces had low input intensity and were highly dependent on the labour force. Then, in the later stages, these provinces experienced two change paths in the pattern of arable land input intensity. Provinces in

Agricultural zoning	Provinces	Stage 1						Stage 2								Stage 3							
		1998	1999	2000	2001	2002	2003	2004	2005	2006	2007	2008	2009	2010	2011	2012	2013	2014	2015	2016	2017	2018	2019
Northeast China Plain	Heilongjiang	50.67	50.25	47.96	45.09	47.84	46.49	52.59	53.75	55.80	52.92	53.27	58.22	62.68	66.03	69.59	71.21	73.29	73.20	60.84	61.24	60.49	55.38
	Jilin	98.57	101.27	87.52	82.74	88.09	95.14	113.87	95.80	100.35	105.96	110.59	115.48	117.68	125.30	129.98	133.37	133.77	134.51	127.04	125.14	123.81	122.25
	Liaoning	118.16	119.70	113.74	103.87	109.28	113.30	117.50	117.45	118.87	125.88	126.84	124.49	125.13	126.62	126.20	130.07	131.31	128.32	122.68	122.05	120.23	116.08
Northern arid and semiarid region	Inner Mongolia	47.64	48.92	49.70	53.95	54.39	61.67	66.43	70.18	75.14	75.64	82.53	90.56	92.42	90.58	95.84	101.87	109.18	108.37	93.52	93.01	90.13	88.02
	Ningxia	112.21	111.54	89.61	93.94	84.31	86.70	90.57	101.11	106.09	107.71	106.46	106.52	111.64	111.46	116.99	117.29	115.78	114.19	128.23	126.98	117.10	118.06
	Gansu	66.64	67.47	68.91	70.94	75.22	75.12	77.29	79.78	79.69	83.48	82.31	82.50	83.88	84.60	88.67	90.02	91.90	90.80	96.21	87.29	85.55	82.21
	Xinjiang	99.41	89.10	89.54	94.09	92.58	97.50	104.15	108.91	117.81	117.12	123.48	124.80	130.03	135.51	138.09	143.11	156.10	156.72	154.56	154.67	152.22	150.48
Huang-Huai-Hai Plain	Beijing	141.85	141.94	153.74	161.36	174.18	184.55	182.10	180.83	172.92	181.01	160.61	162.40	163.06	170.95	179.17	192.19	220.51	225.64	242.99	261.42	261.68	258.93
	Tianjin	112.35	115.07	129.52	131.50	138.66	144.48	177.39	182.57	183.53	226.96	217.95	217.11	207.19	198.39	193.42	193.92	183.63	177.10	180.56	151.19	140.66	142.20
	Hebei	117.83	119.56	119.67	121.32	123.78	130.01	132.17	136.11	136.93	141.71	141.20	143.25	145.22	145.57	146.64	147.93	150.27	146.18	145.40	143.10	137.80	133.13
	Shandong	133.63	137.96	140.00	140.22	144.46	145.77	154.66	158.11	164.26	167.28	159.02	158.23	158.65	157.94	159.27	156.97	155.28	151.47	143.48	141.24	136.22	130.79
	Henan	115.17	118.82	119.86	125.45	130.26	126.93	131.57	135.92	138.75	145.86	152.45	157.87	162.94	166.96	169.33	171.15	172.37	172.36	164.90	164.89	159.71	154.53
Loess Plateau	Shanxi	84.03	85.31	84.56	91.02	89.08	93.82	96.83	97.82	98.75	105.23	105.30	107.24	110.76	112.91	115.56	118.48	116.72	111.33	111.58	105.06	103.11	102.27
	Shaanxi	97.90	102.67	105.02	110.35	110.02	127.06	121.84	125.51	125.32	138.88	139.80	142.21	150.24	168.04	189.13	189.33	181.53	180.35	185.29	188.73	185.58	163.61
Qinghai Tibet Plateau	Qinghai	59.83	53.88	55.35	58.59	63.25	65.20	63.95	65.77	65.20	64.42	67.03	68.94	68.02	67.60	72.07	74.66	76.07	78.00	70.02	69.94	65.23	55.34
	Tibet	73.44	52.20	49.52	58.70	59.95	65.94	69.54	84.42	88.70	94.48	93.99	97.23	98.64	98.48	103.86	117.25	117.74	129.07	128.46	132.82	131.45	130.75
Middle-lower Yangtze Plain	Anhui	107.75	107.96	109.43	115.46	107.57	110.56	107.05	109.64	112.82	119.80	119.76	121.36	123.54	127.58	129.99	132.33	133.17	132.05	129.95	127.65	124.36	118.99
	Jiangsu	154.25	155.72	156.83	160.69	159.76	160.28	161.23	162.84	163.84	168.48	166.03	166.41	163.73	160.95	158.32	155.86	154.88	152.22	151.01	148.19	143.70	142.10
	Jiangxi	68.90	70.07	67.28	69.93	74.23	78.56	84.06	87.57	88.17	90.55	90.43	92.31	93.43	95.57	91.69	88.12	88.52	88.91	86.37	82.91	77.75	73.53
	Hubei	131.30	119.68	120.86	120.96	128.50	138.60	144.10	142.72	144.70	155.33	160.25	162.16	156.67	158.28	157.43	155.18	153.25	150.11	147.54	141.95	131.39	124.81
	Hunan	81.87	81.37	82.63	84.36	86.12	88.52	93.32	94.99	99.75	106.38	106.58	103.33	103.28	103.71	104.87	102.85	101.45	101.25	105.94	105.83	107.31	101.71
	Shanghai	108.70	147.22	145.98	159.55	143.55	143.12	142.20	135.91	135.53	134.11	138.41	114.88	109.39	110.00	104.33	105.12	105.89	109.37	112.84	117.05	112.47	105.48
	Zhejiang	96.60	98.92	105.70	115.50	123.27	130.42	136.59	134.65	132.85	151.83	151.09	150.46	150.30	151.09	159.96	160.30	157.34	152.59	171.31	163.86	154.95	142.09
Sichuan Basin and surrounding	Chongqing	78.32	77.95	79.67	80.64	82.71	84.54	87.79	89.03	94.87	102.57	103.21	103.13	102.12	104.15	103.34	102.45	102.53	101.94	107.62	106.28	104.08	101.76
	Sichuan	81.93	83.68	85.36	85.29	84.35	85.52	87.86	88.96	89.74	96.90	96.67	98.66	98.50	99.00	98.78	97.96	98.63	98.52	99.60	96.20	93.34	87.94
Yunnan-Guizhou Plateau	Guizhou	54.32	56.41	57.92	57.76	60.40	61.80	60.32	61.88	63.19	70.45	69.28	69.19	67.53	71.21	71.92	68.92	70.05	70.36	68.54	63.57	61.72	58.07
	Yunnan	76.71	64.02	73.94	76.98	81.86	85.24	88.15	88.41	91.15	101.18	102.52	99.71	105.33	109.66	110.49	111.29	114.26	116.91	125.46	122.25	112.47	105.05
	Guangxi	81.18	79.39	81.97	85.85	89.40	92.37	96.29	97.37	109.40	122.95	122.88	123.78	126.35	127.50	129.19	131.56	138.32	134.50	138.85	139.79	135.97	134.32
Southern China	Fujian	137.26	143.65	148.67	145.95	151.53	160.16	161.76	164.65	164.49	180.57	177.40	177.63	176.82	175.88	177.40	174.95	176.70	216.26	264.27	249.11	233.02	221.29
	Guangdong	109.11	116.45	120.37	129.65	137.03	140.11	142.84	142.22	144.81	165.73	169.60	171.63	172.72	174.20	174.71	170.86	172.97	176.25	203.58	199.44	178.00	171.05
	Hainan	82.82	69.07	98.58	108.45	110.13	122.38	163.79	155.06	153.95	175.44	181.62	182.78	182.24	185.05	174.02	183.08	186.81	195.21	221.82	232.66	216.35	218.91

Emergy Input per hectare (10^{13}sej/ha): 264.27, 213.13, 154.68, 103.54, 45.09

(a)

Agricultural zoning	Provinces	Yield-enhancing physical inputs (1.00E+13 sej/ha)			Labor inputs (1.00E+13 sej/ha)			Agricultural machinery inputs (1.00E+13 sej/ha)		
		Stage 1(1998-2003)	Stage 2(2004-2011)	Stage 3(2012-2019)	Stage 1(1998-2003)	Stage 2(2004-2011)	Stage 3(2012-2019)	Stage 1(1998-2003)	Stage 2(2004-2011)	Stage 3(2012-2019)
Northeast China Plain	Heilongjiang	44.29	51.88	58.50	0.94	0.75	0.56	2.82	4.27	6.61
	Jilin	86.89	103.52	118.98	1.54	1.26	1.00	3.79	5.85	8.75
	Liaoning	104.04	111.87	113.51	2.97	2.28	1.63	5.99	8.70	9.47
Northern arid and semiarid region	Inner Mongolia	47.73	73.45	89.75	1.12	0.87	0.59	3.87	6.11	7.15
	Ningxia	88.33	94.84	108.58	1.78	1.44	1.19	6.27	8.92	9.56
	Gansu	63.29	72.28	78.10	2.62	2.27	1.76	4.80	7.14	9.22
	Xinjiang	88.21	113.62	142.61	1.30	1.36	1.04	4.19	5.24	7.09
Huang-Huai-Hai Plain	Beijing	139.55	151.83	203.34	4.24	4.28	9.51	15.82	15.63	17.47
	Tianjin	107.31	177.46	150.05	3.45	2.94	2.81	17.84	20.99	17.48
	Hebei	106.14	120.30	124.42	2.87	2.38	1.99	13.01	17.59	17.39
	Shandong	126.79	141.59	128.07	3.03	2.36	1.82	10.53	15.82	16.95
	Henan	112.45	136.30	152.55	2.87	2.16	1.63	7.43	10.58	11.97
Loess Plateau	Shanxi	77.71	90.75	98.36	2.86	2.51	2.13	7.40	11.10	10.03
	Shaanxi	101.77	129.69	171.71	3.00	2.62	1.97	4.06	6.67	9.26
Qinghai Tibet Plateau	Qinghai	46.62	51.41	54.13	3.08	3.12	2.47	8.16	11.84	13.56
	Tibet	46.48	63.68	68.50	4.50	4.48	4.41	8.98	22.52	51.02
Middle-lower Yangtze Plain	Anhui	101.32	107.08	115.09	2.76	2.06	1.62	5.71	8.55	11.85
	Jiangsu	148.72	154.12	138.79	3.17	2.36	1.66	6.03	7.71	10.34
	Jiangxi	65.76	79.30	75.90	2.78	2.42	1.87	2.95	8.53	6.96
	Hubei	120.90	145.06	134.89	2.53	2.08	1.50	3.23	5.88	8.82
	Hunan	76.15	90.82	90.46	3.27	2.45	1.85	4.72	8.15	11.59
	Shanghai	133.35	120.45	98.89	3.51	2.96	4.20	4.50	4.14	5.98
	Zhejiang	96.91	125.75	136.38	5.14	4.48	4.21	9.68	14.63	17.20
Sichuan Basin and surrounding	Chongqing	74.49	91.58	95.84	3.30	2.29	1.61	2.84	4.48	6.30
	Sichuan	77.98	87.17	86.95	3.45	2.73	2.10	2.92	4.63	7.32
Yunnan-Guizhou Plateau	Guizhou	52.62	59.06	58.06	3.24	2.75	1.77	2.24	4.82	6.82
	Yunnan	69.60	90.45	105.77	2.92	2.46	1.82	3.94	5.36	7.18
	Guangxi	78.02	106.84	123.47	3.07	2.51	2.01	3.93	6.46	9.84
Southern China	Fujian	137.89	160.55	198.85	4.68	4.02	3.71	5.31	7.84	11.57
	Guangdong	114.28	148.98	168.01	5.56	4.17	3.62	5.62	7.33	9.23
	Hainan	92.17	162.73	189.85	2.65	2.73	2.49	3.76	7.03	11.26

(b)

44.29 110.88 ≥177.46 | 0.56 3.06 ≥5.56 | 2.24 11.62 ≥20.99

Fig. 3. (a) Provincial total arable land input intensity during 1998–2003. (b) Average value of three types of input intensity (i.e., yield-enhancing physical inputs; labour inputs and agricultural machinery inputs) at the provincial level in stages 1–3. The provinces marked with the green background are the major grain-producing provinces. Yield-enhancing physical input intensity is the summation of fertilizer, pesticide and mulching film input intensity. Hong Kong, Macau and Taiwan are not listed due to lack of data. (For interpretation of the references to colour in this figure legend, the reader is referred to the Web version of this article.)

the western regions where irrigated agriculture dominates mainly show the development from Class B to Class A. In this process, the input intensity of fertilizer and agro-machinery experienced a small increase; the labour force input intensity decreased. Furthermore, this process is also the main reason for the increase in mulching film input intensity. White pollution needs to be controlled in these provinces. For provinces involving the Northeast China Plain, Middle-lower Yangtze Plain and Central Shaanxi Plain, the main form of change is from Class B to Class E. In this process, the input intensity of fertilizer and pesticides experienced a larger increase than the previous change path (i.e., Class B to Class A); the input intensity of mulching film is stable at a low level. The pattern of arable land input intensity is relatively stable in the Huang-Huai-Hai Plain and Southern China. The former is stable at Class C, and the latter is stable at Class D. Reducing the pesticide input intensity and promoting agricultural machinery are key challenges for provinces belonging to Class D to achieve sustainable intensification.

3.4. Coupled relation analysis between input intensity and output intensity

Sliding window-based partial correlation analysis was used to present the local influence of element input intensity change on the output intensity of staple food grains (Fig. 7(a/b/c/d/e−1)) and oil crops (Fig. 7 (a/b/c/d/e−2)). Three groups of samples were tested for each experiment. Group A is the set of all samples. Group B consists of provinces

(a)

Agricultural zoning	Provinces	Stage 1						Stage 2								Stage 3							
		1998	1999	2000	2001	2002	2003	2004	2005	2006	2007	2008	2009	2010	2011	2012	2013	2014	2015	2016	2017	2018	2019
Northeast China Plain	Heilongjiang	6.27	6.23	6.30	6.24	6.21	6.34	6.64	6.55	6.44	6.70	6.95	7.01	6.93	7.04	7.12	7.17	7.23	7.41	7.53	7.19	7.14	7.18
	Jilin	10.18	9.40	5.92	6.46	7.70	7.93	8.21	8.35	8.93	8.04	9.19	8.02	8.84	9.97	10.30	10.55	10.03	10.19	10.50	10.71	9.22	9.85
	Liaoning	8.60	7.78	5.58	6.39	7.47	7.76	8.30	8.09	7.78	8.26	8.65	7.22	7.74	8.93	9.01	9.60	7.53	8.54	9.14	9.55	8.93	9.98
Northern arid and semiarid region	Inner Mongolia	4.53	4.23	3.93	4.08	4.60	4.70	5.03	5.40	5.40	5.24	5.83	5.29	5.68	6.08	6.55	7.09	7.17	7.31	7.13	7.20	7.81	7.92
	Ningxia	5.17	5.20	4.77	5.04	4.97	4.71	5.16	5.36	5.37	5.32	5.25	5.55	5.69	5.79	6.28	6.41	6.91	6.94	7.24	7.25	7.75	8.11
	Gansu	4.50	3.85	3.36	3.55	3.81	3.95	3.94	3.87	3.60	3.49	3.87	3.86	4.13	4.34	4.90	4.97	5.13	5.26	5.14	5.39	5.58	5.78
	Xinjiang	7.41	7.47	7.57	7.84	7.86	7.99	8.02	8.40	8.61	8.91	8.45	8.08	8.11	8.46	8.56	8.79	8.87	9.04	8.97	9.23	9.72	9.94
Huang-Huai-Hai Plain	Beijing	8.13	6.99	6.63	6.99	6.91	5.86	6.51	7.15	7.18	7.49	8.07	8.05	7.57	8.52	8.59	8.90	7.84	8.81	9.05	9.12	9.07	9.15
	Tianjin	6.64	5.70	6.27	6.34	6.39	6.66	6.74	6.89	7.01	7.24	7.28	7.30	7.36	7.49	7.22	7.61	7.35	7.47	7.89	8.57	8.42	9.23
	Hebei	5.84	5.60	5.36	5.47	5.46	5.81	6.07	6.16	6.40	6.73	6.89	6.87	6.91	7.36	7.48	7.72	7.71	7.64	8.03	8.38	8.17	8.38
	Shandong	7.06	7.14	7.12	7.04	6.50	7.26	7.77	8.09	8.24	8.33	8.53	8.55	8.52	8.63	8.74	8.65	8.61	8.80	8.78	9.08	9.03	9.16
	Henan	5.05	5.16	4.31	4.34	4.69	4.09	4.67	4.47	4.55	4.28	5.18	5.12	5.84	6.47	6.69	6.93	7.20	7.20	6.92	6.95	7.18	7.13
Loess Plateau	Shanxi	4.81	3.88	3.73	3.56	4.43	5.00	5.53	4.90	5.26	5.21	5.47	4.84	5.39	5.77	6.13	6.31	6.36	6.02	6.25	6.60	6.78	6.70
	Shaanxi	4.49	3.80	3.93	3.87	4.06	4.20	4.54	4.50	4.53	4.84	4.97	5.08	5.15	5.32	5.57	5.48	5.44	5.63	5.62	5.57	5.76	5.80
Qinghai Tibet Plateau	Qinghai	4.50	3.81	2.96	3.65	3.55	3.59	3.78	3.99	3.61	4.66	3.92	3.81	3.99	4.10	4.15	2.88	4.18	4.21	4.08	4.09	4.09	4.42
	Tibet	6.69	7.24	7.49	7.64	7.61	8.11	8.11	7.84	8.26	8.50	8.81	8.65	8.58	8.67	8.43	8.34	8.33	8.46	8.16	7.63	8.40	7.70
Middle-lower Yangtze Plain	Anhui	5.15	5.57	4.87	5.34	5.52	4.36	5.38	5.06	5.60	5.77	5.97	6.02	6.04	6.16	6.49	6.49	6.77	7.00	7.05	7.04	7.20	7.33
	Jiangsu	7.25	7.73	7.34	7.56	7.47	6.66	7.46	7.26	7.70	7.63	7.66	7.78	7.79	7.91	8.04	8.12	8.29	8.38	8.12	8.40	8.56	8.83
	Jiangxi	5.23	5.64	5.59	5.64	5.60	5.47	5.73	5.89	6.06	6.22	6.31	6.41	6.20	6.50	6.56	6.62	6.69	6.69	6.69	6.82	6.84	6.83
	Hubei	5.89	6.33	6.10	6.30	6.32	5.45	6.44	6.81	7.39	7.68	7.74	7.72	7.74	7.80	7.86	7.90	7.87	8.24	8.05	8.40	8.60	8.77
	Hunan	6.03	6.15	6.36	6.48	6.17	6.21	6.42	6.37	6.49	6.90	7.12	7.05	6.90	7.04	7.15	6.90	7.03	7.09	7.06	7.26	7.48	7.59
	Shanghai	7.57	7.78	8.28	8.82	8.59	8.11	8.42	7.83	8.28	7.95	8.20	7.94	8.25	8.15	8.25	8.49	8.55	8.64	8.72	9.10	9.67	9.72
	Zhejiang	6.02	5.87	6.14	6.38	6.60	6.44	6.63	6.20	6.70	7.04	7.09	7.11	7.03	7.24	7.13	6.79	6.93	6.78	6.84	6.90	7.14	7.11
Sichuan Basin and surrounding	Chongqing	4.20	4.18	4.36	4.04	4.45	4.76	4.95	5.04	5.22	5.33	5.59	5.44	5.49	5.33	5.35	5.40	5.39	5.44	5.50	5.60	5.62	5.65
	Sichuan	5.91	5.99	6.14	5.41	5.99	6.11	6.07	6.07	5.25	5.66	5.81	5.86	5.97	6.05	6.08	6.24	6.22	6.33	6.44	6.55	6.58	6.58
Yunnan-Guizhou Plateau	Guizhou	4.22	4.28	4.37	4.15	3.92	4.24	4.39	4.35	4.20	4.57	4.64	4.58	4.35	3.09	4.00	3.63	3.96	4.13	4.18	4.63	4.08	4.03
	Yunnan	4.50	4.57	4.70	4.43	4.33	4.55	4.44	4.46	4.50	4.59	4.74	4.81	4.63	4.99	5.17	5.22	5.23	5.30	5.38	5.82	5.87	5.89
	Guangxi	4.91	5.01	4.97	4.92	4.95	5.00	4.74	5.08	5.24	5.59	5.61	5.69	5.51	5.58	5.81	5.93	6.00	5.98	6.04	5.88	5.99	5.93
Southern China	Fujian	4.97	4.92	4.85	4.91	4.81	4.97	5.11	5.09	5.12	5.59	5.68	5.69	5.63	5.75	5.78	5.80	5.81	5.76	5.73	6.27	6.39	6.38
	Guangdong	6.04	6.39	5.81	5.58	5.60	5.63	5.42	5.44	5.44	5.67	5.44	5.69	5.70	5.91	6.05	5.76	5.95	5.95	5.96	6.28	6.25	6.47
	Hainan	3.80	3.95	3.79	3.92	3.78	3.74	4.18	3.64	4.38	4.60	4.57	4.57	4.33	4.61	4.84	4.86	4.93	5.09	5.15	5.31	5.56	5.68

Energy output per ha. (1.0E+07kJ/ha)
10.71
8.89
6.80
4.97
2.88

(b)

Agricultural zoning	Provinces	Stage 1						Stage 2								Stage 3							
		1998	1999	2000	2001	2002	2003	2004	2005	2006	2007	2008	2009	2010	2011	2012	2013	2014	2015	2016	2017	2018	2019
Northeast China Plain	Heilongjiang	7.11	6.59	7.07	7.06	6.02	6.70	7.88	7.45	7.65	8.05	7.74	8.05	8.04	7.99	7.99	8.29	8.36	8.45	8.61	8.83	8.91	9.09
	Jilin	6.46	7.01	5.30	5.43	10.82	7.01	6.35	6.99	7.51	4.37	9.04	7.68	8.60	10.50	11.21	11.24	11.91	10.51	10.36	11.64	11.54	11.76
	Liaoning	7.06	6.00	5.48	7.27	6.83	6.79	6.80	6.71	8.92	9.59	10.17	9.53	10.61	10.31	10.36	10.37	9.45	8.53	10.82	10.83	9.94	12.32
Northern arid and semiarid region	Inner Mongolia	5.89	5.49	4.90	4.91	5.85	5.23	5.72	6.51	6.55	6.69	7.09	7.49	7.37	6.91	7.02	7.21	7.31	7.84	7.93	8.00	8.37	9.09
	Ningxia	2.86	3.21	3.30	2.71	3.64	3.68	4.09	4.66	4.68	5.61	6.23	5.89	7.81	7.68	7.55	7.58	7.62	7.49	7.93	7.72	8.01	7.31
	Gansu	5.05	4.78	4.94	4.35	4.99	5.09	5.40	5.66	5.58	5.63	5.97	6.16	6.86	6.70	7.37	7.66	8.15	8.27	8.47	8.26	8.00	8.07
	Xinjiang	6.55	6.84	7.18	7.25	7.63	8.20	7.65	7.77	8.01	7.66	7.34	8.76	9.02	9.35	9.02	10.12	9.96	10.66	11.00	10.87	11.20	11.24
Huang-Huai-Hai Plain	Beijing	10.83	9.82	9.13	11.20	10.95	8.84	9.92	10.73	11.13	11.56	11.16	11.00	10.64	10.52	11.03	10.63	9.58	9.97	9.37	9.15	9.64	9.25
	Tianjin	6.93	5.35	4.66	7.05	6.66	7.22	9.42	9.39	9.66	9.52	9.87	10.02	10.83	11.16	11.00	11.83	11.35	12.02	8.84	8.33	11.04	13.46
	Hebei	8.12	7.55	7.92	9.01	8.72	9.52	9.79	10.11	10.34	10.26	10.93	10.68	11.18	11.58	11.64	11.89	11.92	12.15	12.37	12.14	12.21	12.13
	Shandong	14.46	13.27	13.81	13.85	12.80	13.22	14.48	14.97	15.23	15.51	15.85	16.10	15.99	16.16	16.30	16.28	16.08	15.82	15.98	16.24	16.17	15.68
	Henan	2.98	4.96	4.47	4.44	5.23	3.57	4.14	5.47	5.43	5.04	4.82	5.13	6.09	5.80	7.10	7.21	7.27	7.17	7.15	6.92	8.06	8.25
Loess Plateau	Shanxi	4.48	2.55	3.98	2.16	4.00	4.17	3.50	2.88	3.15	3.55	3.95	3.71	4.15	4.62	4.96	5.14	4.94	4.67	4.98	4.88	5.12	5.08
	Shaanxi	4.61	3.83	4.72	4.77	5.42	5.36	6.02	6.06	6.14	5.75	6.60	6.81	6.89	7.26	7.39	7.37	7.67	7.76	7.75	7.94	7.94	8.12
Qinghai Tibet Plateau	Qinghai	5.27	5.48	3.75	5.05	5.66	6.38	6.69	7.28	6.15	6.89	7.55	7.86	7.15	7.34	7.93	7.61	7.73	7.79	7.80	7.22	7.12	7.52
	Tibet	6.53	8.92	9.10	9.59	8.21	8.48	8.19	8.70	8.38	8.37	9.04	8.74	9.04	9.79	9.76	9.63	9.63	9.96	10.18	11.22	9.63	9.81
Middle-lower Yangtze Plain	Anhui	5.33	7.43	7.24	7.81	7.19	6.06	8.04	7.69	8.38	8.53	9.01	9.18	8.92	9.01	9.99	10.40	10.74	10.92	10.88	11.04	11.24	11.31
	Jiangsu	6.83	9.50	9.31	9.28	8.85	8.10	9.58	9.44	9.94	9.93	9.80	10.12	9.79	9.65	10.31	10.74	10.87	11.14	11.58	11.81	12.12	12.32
	Jiangxi	3.29	3.88	4.17	4.30	4.33	4.44	4.87	4.88	4.93	5.07	5.12	5.27	5.44	5.74	5.82	5.94	6.07	6.20	6.19	6.39	6.57	6.60
	Hubei	9.35	9.82	9.73	9.29	10.13	9.90	9.83	10.36	11.43	12.09	12.57	13.20	13.33	13.14	14.24	14.73	14.69	15.21	15.63	15.54	15.98	15.58
	Hunan	4.90	5.15	5.52	5.57	4.94	5.36	5.89	5.81	6.02	5.87	5.33	5.87	5.97	6.15	5.82	6.01	6.07	6.22	6.25	6.38	6.45	6.48
	Shanghai	4.37	8.13	8.47	7.43	6.83	6.00	8.72	8.00	8.18	8.21	8.60	8.09	8.24	8.02	7.81	8.15	8.28	8.60	7.91	8.80	9.41	10.57
	Zhejiang	4.67	6.92	6.79	7.03	6.01	6.46	7.61	7.44	7.44	8.06	8.01	7.62	7.00	7.53	7.48	7.62	7.83	7.94	7.63	8.14	8.48	8.41
Sichuan Basin and surrounding	Chongqing	4.83	4.52	5.08	4.93	5.49	5.98	6.33	6.26	5.80	5.89	6.13	6.33	6.45	6.70	6.84	6.94	7.02	7.16	7.25	7.25	7.25	7.31
	Sichuan	6.48	6.30	6.96	6.38	7.11	7.39	7.68	7.85	7.51	7.95	8.06	8.10	8.19	8.40	8.54	8.52	8.69	8.80	8.89	8.96	9.01	9.09
Yunnan-Guizhou Plateau	Guizhou	5.14	5.12	5.37	5.30	5.31	5.33	5.76	5.65	5.87	5.95	5.56	5.29	5.55	5.44	5.91	6.04	6.23	6.35	6.44	6.47	6.39	6.37
	Yunnan	4.53	4.86	4.70	5.13	5.47	5.79	6.04	5.95	6.37	6.01	5.98	5.85	6.29	6.57	6.77	6.28	6.66	6.85	7.13	7.21	7.29	7.36
	Guangxi	5.69	5.88	6.35	6.45	6.64	6.84	7.05	7.45	7.61	8.19	8.51	8.59	8.79	9.16	9.28	9.54	9.57	9.64	9.92	10.04	10.14	10.45
Southern China	Fujian	7.61	7.86	7.64	7.80	7.85	7.80	8.23	8.29	8.21	8.50	8.75	8.81	8.91	9.13	9.27	9.40	9.59	9.73	9.78	9.98	10.43	10.51
	Guangdong	8.24	8.45	8.48	8.47	8.70	9.07	9.07	8.96	9.09	9.26	9.32	9.45	9.67	9.91	10.15	10.38	10.64	10.87	11.06	11.30	11.53	11.71
	Hainan	6.29	6.62	6.90	6.98	6.95	7.15	7.10	7.06	7.73	7.70	8.00	8.28	8.63	9.10	9.66	10.00	10.60	10.39	10.34	10.13	9.89	10.19

Energy output per ha. (1.0E+07kJ/ha)
16.30
13.00
9.23
5.93
2.16

Fig. 4. Provincial annual output intensity of (a) staple food grains and (b) oil crops during 1998–2019. The provinces marked with the green background are the major grain-producing provinces. Hong Kong, Macau and Taiwan are not listed due to lack of data. (For interpretation of the references to colour in this figure legend, the reader is referred to the Web version of this article.)

with high levels of crop output. Group C involves mountainous or plateau provinces.

As Fig. 7(a-1) shows, fertilizer input intensity shows a significant ($p < 0.001$) positive correlation with the output intensity of staple food grains at a low input level, especially for Group C. This correlation is gradually decoupled (i.e., becomes nonsignificant ($p > 0.05$)) as the fertilizer input intensity increases. The inflection point first occurs in the normalized value segment of [32.592, 71.743] and last four sliding windows to [42.657, 80.969] (note: [35.596, 73.332] presents the minimum and maximum values of samples in a specific sliding window, corresponding to a specific point in Fig. 7(a-1), whose x-coordinate is equal to the average value of these samples). Then, the input intensity of fertilizer was recoupled with the output intensity with a significant ($p < 0.001$) negative correlation. This demonstrates that superfluous fertilizer inputs have hampered agricultural output in some provinces of China. The appropriate fertilizer input intensity is below the normalized value of 32.592 (the corresponding input intensity of fertilizer is 9.27 E+14 sej/ha.). The non-significant ($p > 0.05$) results of Group C in the high input intensity range are mainly due to insufficient sample quantity. According to Fig. 7(a-2), the increase in fertilizer input intensity promotes the synergetic increase in its significant ($p < 0.001$) positive correlation with the output intensity of oil crops in the initial stage. The significant positive correlation lasts until the normalized value segment of [42.66, 80.97]. This illustrates that oil crops show higher dependence on fertilizer than staple food grains because the former maintains a positive correlation over a longer range of input intensities. For Group C, the correlation between fertilizer input intensity and output intensity of oil crops remains significantly ($p < 0.05$) positive until the normalized value segment of [55.26, 93.62].

The change in the local partial correlation coefficient between pesticide input intensity and output intensity of staple food grains with pesticide input intensity (Fig. 7(b-1)) is similar to Fig. 7(a-1) for Groups A and B. The difference is that pesticide input intensity shows a larger decoupling gradient than that of fertilizer. The inflection point first

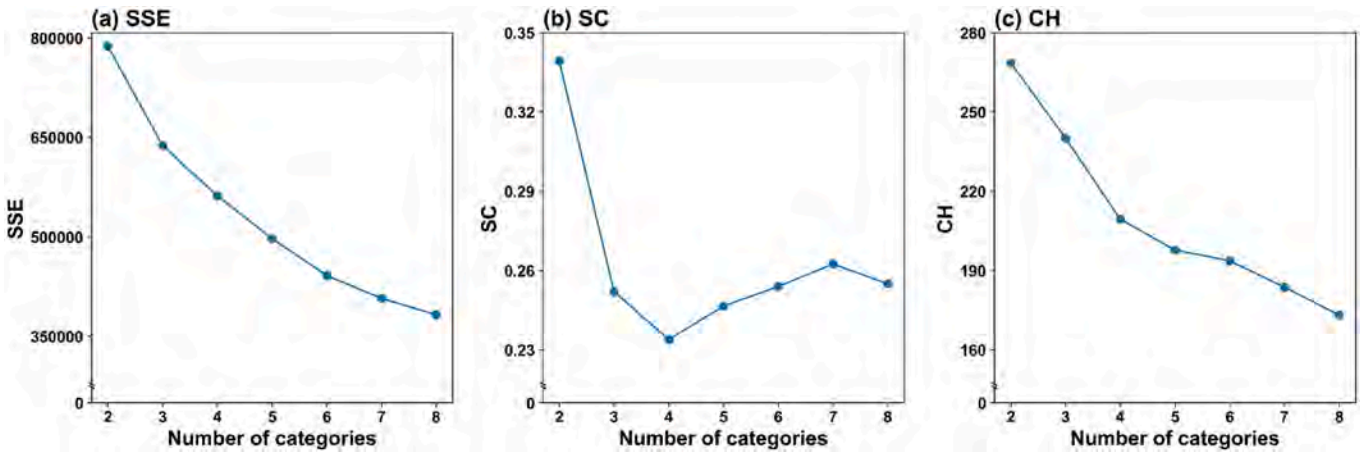

Fig. 5. The sum of squares due to error (abbr. SSE) index, silhouette score (abbr. SC) index and Calinski-Harabaz (abbr. CH) index in multiple classification schemes with different numbers of categories.

occurs in the normalized input intensity value segment of [17.54, 57.30]. This demonstrates that superfluous pesticide input is more common than fertilizer input. This is because precise prevention of agricultural pests and diseases is difficult, which makes pesticides an important safeguard against risk. For Group C, pesticide input intensity shows persistent negative effects on the output intensity of staple food grains. According to Fig. 7(b-2), the change in the local partial correlation coefficient between pesticide input intensity and output intensity of oil crops with pesticide input intensity shows consistency among the three groups. The pesticide input intensity shows larger negative effects on the output intensity of oil crops than that of staple food grains since the local partial correlation coefficients in Fig. 7(b-2) are obviously lower than those in Fig. 7(b-1).

In mountainous or plateau provinces (i.e., Group C), the coupling relationship between mulching film input intensity and output intensity of staple food grains has experienced three states in turn: coupling with significant ($p < 0.01$) negative correlation—decoupling (i.e., non-significant)—recoupling with significant ($p < 0.05$) positive correlation (Fig. 7(c-1)). In these provinces, the target of increasing output intensity puts forwards high requirements for the input intensity of film mulch. For Group C, the recoupling high positive correlation shows that the mulching film input intensity is not yet saturated and explains the continuous increase in mulching film input intensity in Fig. 2(f). The mulching film input intensity may further increase without appropriate controls. Group B shows the opposite change in the coupling relationship between mulching film input intensity and output intensity of staple food grains. The conflict between Group C and Group B on the local partial correlation coefficient change rule leads to a general nonsignificant correlation for Group A. The local influence change of mulching film input intensity to oil crop output intensity (Fig. 7(c-2)) is similar to Fig. 7(c-1).

As Fig. 7(d-1) and 7 (d-2) show, the agro-machinery input intensity presents a continuous significant positive correlation with two types of output intensity for Group A. For Group C, the agro-machinery input intensity shows a significant high positive correlation to the output intensity of staple food grains, but its positive correlation to the output intensity of oil crops is much weaker. Provinces in Group B show superfluous agricultural mechanical power since the increased agro-machinery input intensity does not promote output intensity. Another reason is that high arable land fragmentation limits the effectiveness of agricultural mechanical power. Arable land fragmentation can also explain the significant high negative correlation between agro-machinery input intensity and two types of output intensity for Group B. For instance, the Northeast China Plain, which shows a relatively low degree of arable land fragmentation, achieves high output intensity with lower agro-machinery input intensity than the Middle-lower Yangtze Plain.

In the low value segment of normalized labour force input intensity ([0, 64.45]), its coupling relationship to two types of output intensity is significantly negatively correlated for all groups (Fig. 7(e−1), 7 (e−2)). This is because in this low value segment, labour force input intensity shows a significant negative correlation to agro-machinery input intensity (Fig. 7(f)), namely, the dependence on labour force for crop production is replaced by agro-machinery and thereby achieves higher output intensity. In the high value segment of normalized labour force input intensity ([30.12, 88.27]), its coupling relationship to two types of output intensity turns to a significant positive correlation. This demonstrates that the dependence on the labour force for crop production is high in agricultural labour-intensive areas, especially for staple food grain production in mountainous or plateau provinces (i.e., Group C in Fig. 7(e−1)). In this high value segment, agro-machinery input intensity shows synergetic development with labour force input intensity (Fig. 7 (f)).

4. Discussion

4.1. Estimate the impact degree of input factors on output intensity

In recent years, the random forest model has become a popular method to capture the nonlinear driving effect of multiple independent variables on dependent variables. In this study, the impact of the input intensity of five elements (i.e., fertilizer; labour force; mulching film; pesticide; agro-machinery) to staple food grain output intensity was quantitatively estimated using the random forest model for each stage (see Appendix B.5 for details on the method). Twenty tests were executed for each stage. The R^2 values of the model fit of the three stages are [0.9618, 0.9702], [0.9719, 0.9786], and [0.9816, 0.9872], respectively (see Appendix B.6 for details on the R^2 value). This result indicates that the fitting effect of the established random forest regression model can accurately explain the impact of each element on output intensity. The impact of the five elements on output intensity is indicated by the increase in mean squared error (Inc. MSE; Fig. 8). The results show that fertilizer input intensity stably plays the most important role in improving output intensity. Although pesticide input intensity dropped sharply in stage 3 (Fig. 2(c)), its importance continued to increase from stage 1 (1998–2003) to stage 3 (2012–2019) and rose to second place in the last stage. Mulching film input intensity has experienced a continuous decline in its influence on output intensity. The importance of agro-machinery input intensity and labour force input intensity shows opposite changes. In stage 1, labour force input intensity plays a much more important role in output intensity than agro-machinery input intensity. Then, during stage 1 to stage 2, the dependence of output

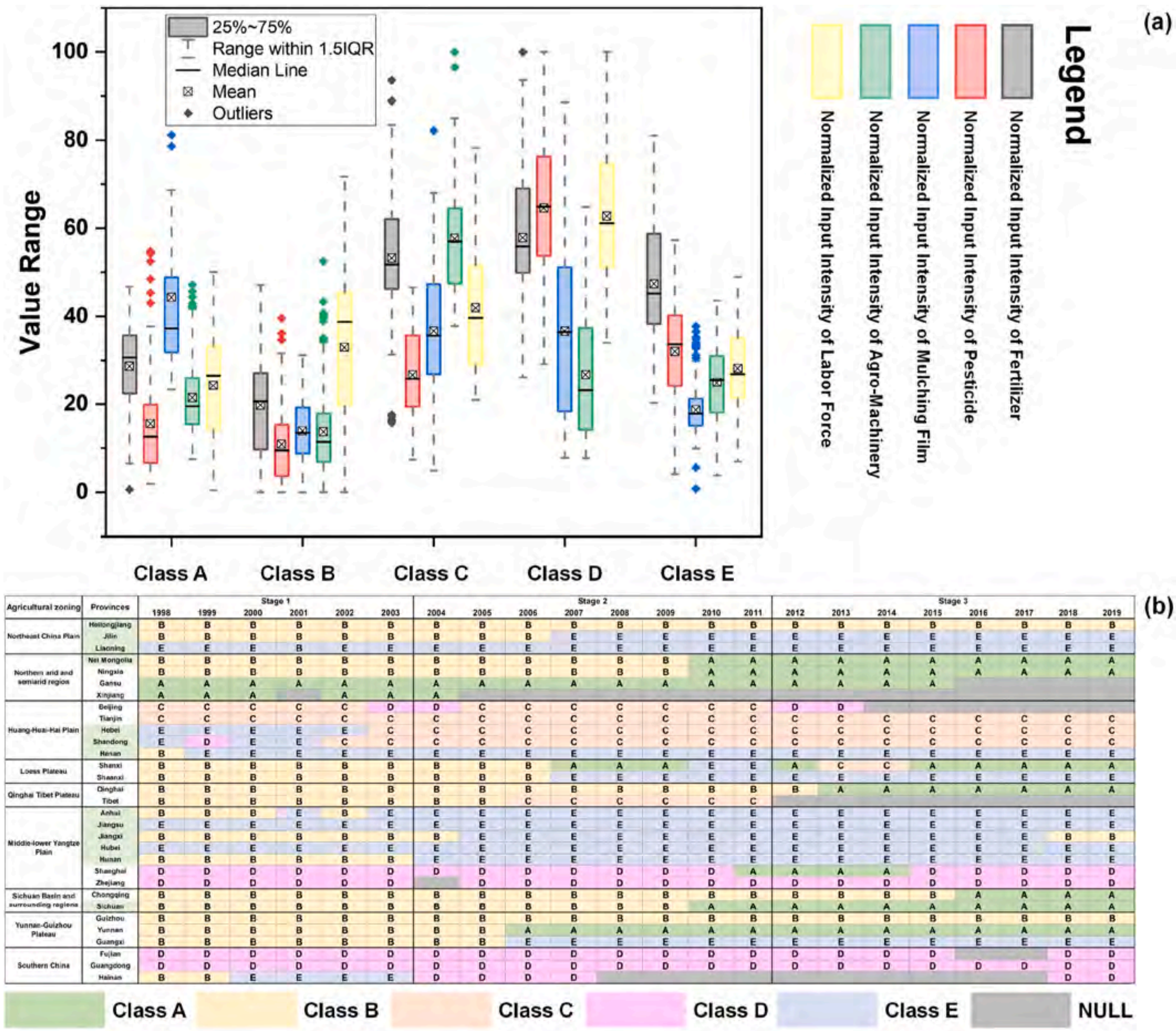

Fig. 6. Structure pattern of provincial annual normalized arable land input intensity. (a) The characteristics of each class on input intensity of fertilizer, pesticides, agro-machinery, labour force and mulching film. (b) Spatial-temporal variation in the structural pattern of arable land input intensity from 1998 to 2019. The provinces marked with the green background are the major grain-producing provinces. Hong Kong, Macau and Taiwan are not listed due to lack of data. Class A–E express the same meaning in (a) and (b). The NULL data in (b) are due to the dramatic change in the provincial input intensity of some elements and are considered outliers. (For interpretation of the references to colour in this figure legend, the reader is referred to the Web version of this article.)

intensity on the labour force is partly replaced by agro-machinery. During stage 2 to stage 3, labour force input intensity becomes the core influencing element of output intensity. In the meantime, the importance of agro-machinery input intensity declines sharply. This phenomenon can be explained by Fig. 7(d-1) and Fig. 7(e−1). In stage 3, the agro-machinery input intensity increases to a superfluous level, which weakens its positive correlation to output intensity (Fig. 7(d-1)). In the same stage, labour force input intensity decreases continuously (Fig. 2(e)), and the negative correlation between labour force input intensity and output intensity increases sharply (Fig. 7(e−1)). The random forest model-based results can reveal the overall driving effect of input elements on output but cannot explain how the input intensity of elements influences output intensity and why their importance changes. The coupled relation analysis of this study can complement it by providing element action process information.

4.2. *Estimate suitability of provincial arable land input intensity*

According to the coupling—decoupling—recoupling process between fertilizer (or pesticide) input intensity and output intensity (Fig. 7), an early warning threshold and critical warning threshold were designed. Then, the suitability of provincial arable land input intensity for fertilizer and pesticide use was divided into three states for each year. The “S” state indicates that the increase in input intensity can significantly promote output intensity (input intensity less than the early warning threshold). The “T” state indicates a nonsignificant correlation between input intensity and output intensity (input intensity is between the early warning threshold and critical warning threshold). The “N” state indicates superfluous input intensity (input intensity higher than the critical warning threshold). For fertilizer input intensity, the early warning threshold and critical warning threshold are 9.27 and 11.9 (unit: 10^{14} sej/ha), respectively. For pesticide input intensity, the early

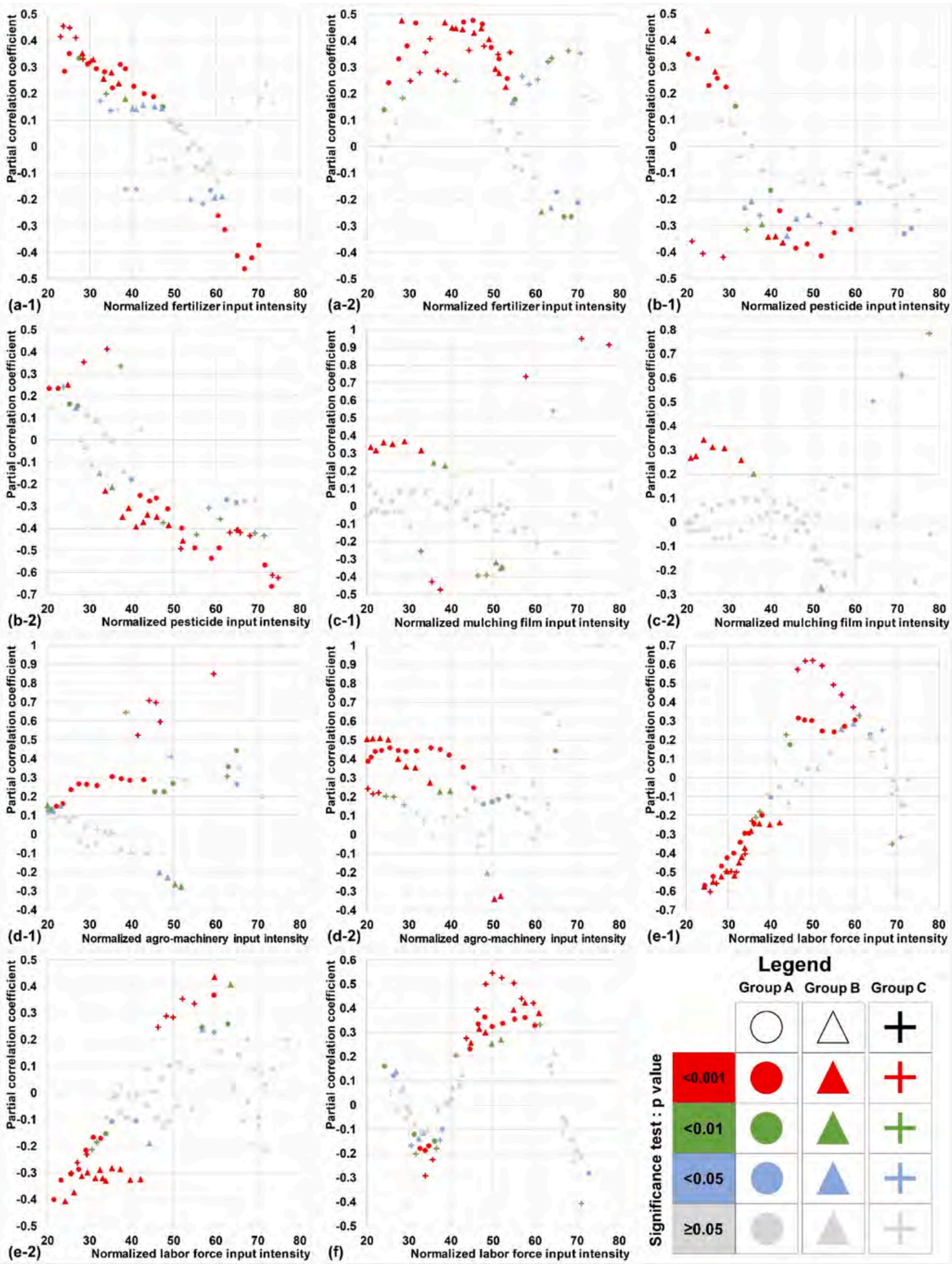

(caption on next page)

Fig. 7. (a/b/c/d/e−1) Local partial correlation coefficients between the input intensity of fertilizer (a-1)/pesticides (b-1)/mulching film (c-1)/agro-machinery (d-1)/labour force (e−1) and the output intensity of staple food grains in different sliding windows. (a/b/c/d/e−2) Local partial correlation coefficients between the input intensity of fertilizer (a-2)/pesticides (b-2)/mulching film (c-2)/agro-machinery (d-2)/labour force (e−2) and the output intensity of oil crops in different sliding windows. (f) Correlation coefficients between labour force input intensity and agro-machinery input intensity in different sliding windows. Three groups of samples were tested for each experiment. Group A is the set of all samples. Group B consists of provinces with high levels of crop output. Group C involves mountainous or plateau provinces. The y-coordinate of each point corresponds to the local partial correlation coefficient between variable ***v*** and the output intensity of a set of samples in a specific sliding window, and its x-coordinate is equal to the average value of ***v*** of these samples. The ***v*** corresponds to the input intensity of a specific element (i.e., fertilizer; pesticides; mulching film; agro-machinery; labour force).

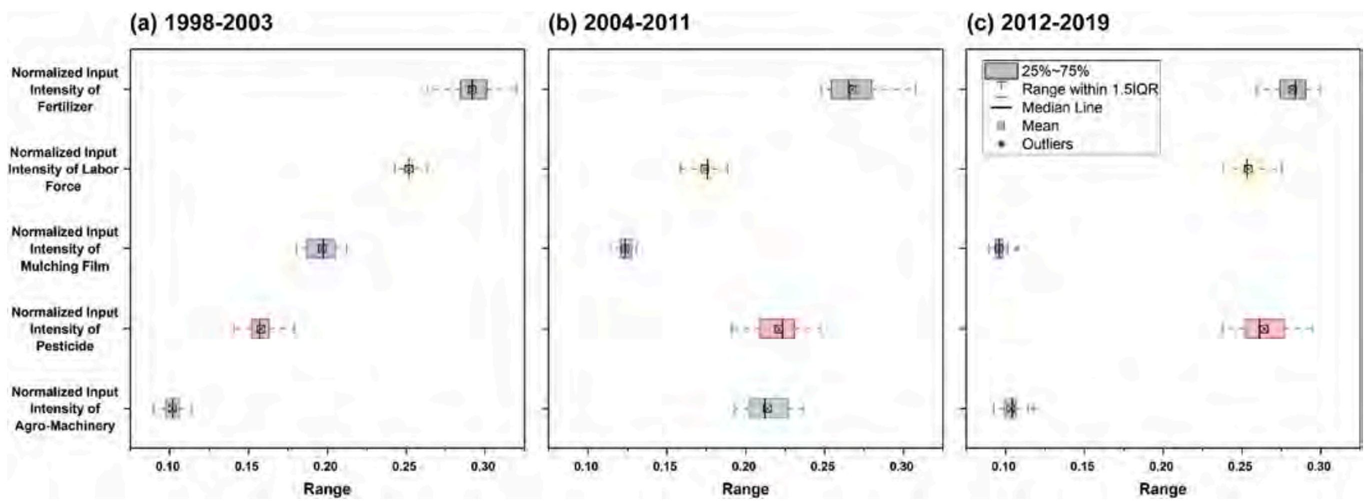

Fig. 8. Estimation of the impact of the input intensity of five elements (i.e., fertilizer; labour force; mulching film; pesticide; agro-machinery) to staple food grain output intensity by using the random forest model and the increase in mean squared error (Inc. MSE) in stages 1–3. Twenty tests were executed for each stage.

warning threshold and critical warning threshold are 1.12 and 1.5 (unit: 10^{13} sej/ha), respectively. The provincial state of each stage is subjectively determined by the overall situation of multiple annual provincial states for years that belong to the stage (Fig. 9).

In stage 1 (Fig. 9(a)), superfluous fertilizer input intensity was mainly distributed in eastern coastal provinces such as Shandong, Jiangsu and Fujian. In the North China Plain and the Middle-Lower Yangtze Plain, the fertilizer input intensity of multiple provinces exceeded the early warning threshold. In stage 2 (Fig. 9(b)), the phenomenon of superfluous fertilizer input intensity worsens, and all "T" state provinces in stage 1 change to the "N" state; Zhejiang turns to the "N" state from the "S" state; the effectiveness of enhancing fertilizer input intensity is lost in Jilin, Sinkiang and Guangxi. In stage 3 (Fig. 9(c)), the phenomenon of superfluous fertilizer input intensity is still spread westwards to Ningxia, Sinkiang and Yunnan, and the states of eastern and central provinces are basically stable compared with stage 2. The suitability of pesticide input intensity also shows obvious east–west differences. In stage 1 (Fig. 9(d)), superfluous pesticide input intensity is more serious and widespread than that of fertilizer. In the later stages, the suitability of pesticide input intensity deteriorates in Gansu, Jilin and Yunnan; southeast provinces remain stable in "N" state; only the state of Hebei is reversed from "N" to "T".

On the whole, although the "zero growth action for fertilizers and pesticides" has made considerable achievements in reducing the input intensity of fertilizer and pesticides since 2015, the severe situation of superfluous fertilizer and pesticide input has not changed substantially. The input intensity of fertilizer and pesticides still needs to be further reduced. Heilongjiang is the only province that shows a stable "S" state on fertilizer and pesticide input intensity compared to other provinces with large plain areas. This demonstrates that soil improvement and an increase in the agricultural operations scale play an important comprehensive role in reducing the input intensity of fertilizer and pesticides.

4.3. Analysing the sustainable intensification status of China from a global perspective

To show the sustainable intensification status of agriculture in China from a global perspective, national arable land use intensity was estimated from three dimensions: output intensity, fertilizer input intensity and pesticide input intensity in 1995, 2000, 2005, 2010, 2015 and 2019 by using a bubble diagram (Fig. 10).

First, from an overall perspective, national output intensity around the world generally increased, while fertilizer input intensity decreased from 1995 to 2019. This demonstrates that global efforts to achieve "zero hunger" and protect farmland ecosystems have paid off. There are significant correlations ($p < 0.01$) between output intensity and fertilizer (or pesticide) input intensity. It also demonstrates that the ratio of output intensity and input intensity is not suitable to indicate the degree of SI at large scales because the output intensity and input intensity may both be extremely low for countries showing extremely high ratios of output intensity and input intensity.

Second, countries leading the world in sustainable intensification of agriculture are mainly in Europe. The countries with output intensities above 8.0 (unit: 1.0 E+7 kJ/ha) are almost all in Europe (e.g., UK, Germany, France, Denmark, Belgium, Luxembourg, and Ireland). In part of them (i.e., Denmark, Germany, Austria, Sweden, etc.), high mechanical input makes crop output less dependent on fertilizers and pesticides and is suitable for promoting "land sharing". However, there are exceptions. For instance, the high output intensity of the Netherlands was highly dependent on fertilizer input before 1995, and this dependence decreased sharply in the following decade. High fertilizer input intensity did not bring high output intensity in Finland, Norway, Belarus, or Iceland. After 2010, fertilizer input intensity continued to decline in Belarus and Finland. The output intensity of Romania, Albania, Ukraine and Portugal has increased rapidly in the last 10 years, with stable low fertilizer input intensity. In addition, pesticide input intensity in the Netherlands and Malta exceeded 90.1 % of all countries in the world in 2019.

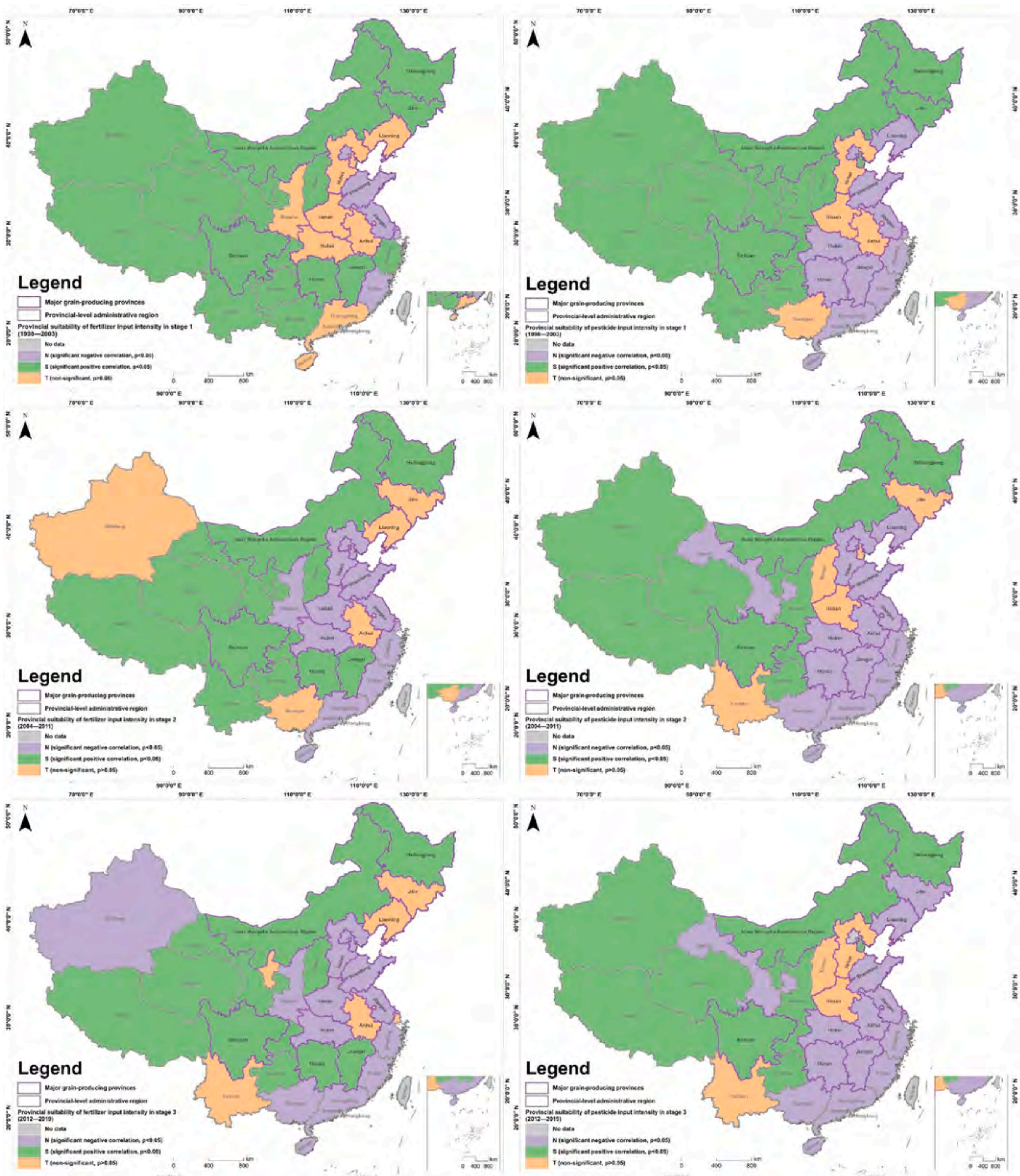

Fig. 9. Estimated suitability of provincial arable land fertilizer (a–c) and pesticides (d–e) input intensity in stages 1–3. The “S” state indicates that the increase in input intensity can significantly promote output intensity. The “T” state indicates a nonsignificant correlation between input intensity and output intensity. The “N” state indicates superfluous input intensity. Hong Kong, Macau and Taiwan have no data.

Third, in the American continents, the output intensity of the United States, Uruguay and Brazil is high with relatively low input intensity of fertilizer and pesticides. Despite the high pesticide input intensity, the SI of Barbados should be taken seriously because it has experienced a process of increasing output intensity with decreasing fertilizer input intensity in the last 10 years. For the Bahamas, Belize, Costa Rica and Saint Lucia, the large increase in fertilizer input intensity and the continuous high pesticide input intensity in the last 10 years do not bring

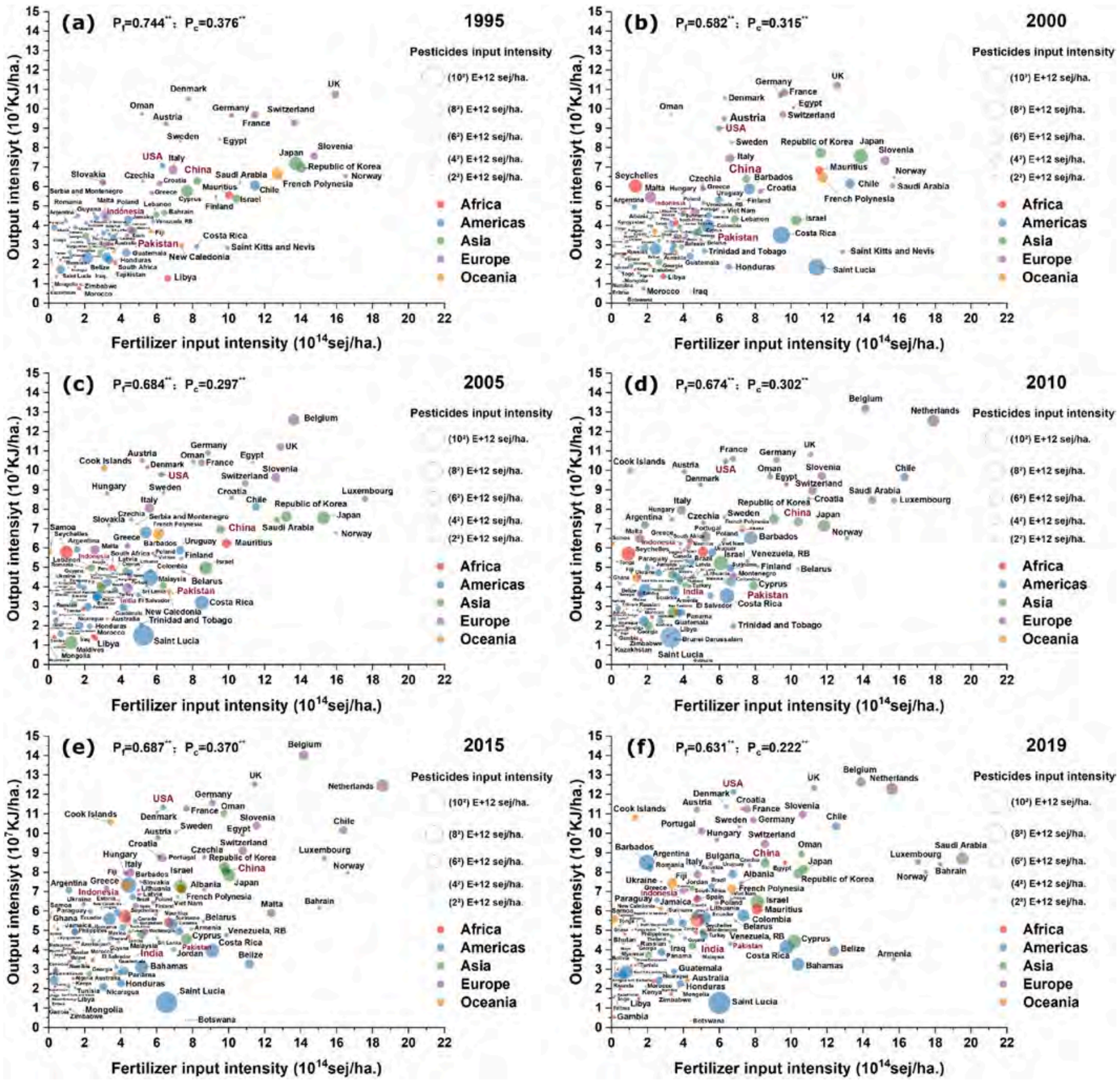

Fig. 10. Pattern of national sustainable intensification of agriculture from three indicators: output intensity, fertilizer input intensity and pesticide input intensity. All indicators are expressed in units of energy. The output intensity is calculated as the annual average output of five primary grain crops (i.e., Corn; Wheat; Beans; Potatoes; Oryza sativa) (unit: kJ/ha.). The fertilizer (or pesticide) input intensity is calculated as annual fertilizer (or pesticide) input per unit area (unit: sej/ha.). Pf (or Pc) presents the Pearson correlation index between output intensity and fertilizer (or pesticide) input intensity. ** indicates p value < 0.01. In the bubble diagram, the x-coordinates and y-coordinates of the circles' centre are set as the fertilizer input intensity and output intensity, respectively; the circles' size is set as the pesticide input intensity. Countries on different continents have been assigned different colours. It should be noted that to clearly show the agricultural intensification features of most countries, the authors have limited the range of the coordinate axes, which makes some countries invisible in specific years (e.g., the Netherlands in 1995, 2000 and 2005). Samples that deviate more than three standard deviations from the mean value are considered outliers. (For interpretation of the references to colour in this figure legend, the reader is referred to the Web version of this article.)

about an increase in output intensity.

Fourth, China nearly achieves the highest level of fertilizer input intensity and output intensity in Asia, which is similar to Japan and the Republic of Korea. Since 2015, China has embarked on a sustainable intensification route with decreasing fertilizer and pesticide input intensity and increasing output intensity. However, this starting point is later than that of the United States, Germany, Austria and France. There is still an obvious gap between the output intensity of China and the world's leading level. Part of the reason is that a mass of low-quality arable land has been cultivated in China to ensure the food demand of her huge population. This poses a huge challenge to enhancing the arable land output intensity of China. Developing and disseminating land consolidation techniques and thereby improving arable land quality is of great significance for China to achieve the world's highest SI level.

Fifth, for most African countries, output intensity, fertilizer input intensity and pesticide input intensity are at low levels, showing great potential for improvement. Egypt and South Africa have explored a sustainable intensification path featuring low fertilizer and pesticide input intensity and high output intensity. Promoting sustainable intensification in African countries plays an important role in achieving sustainable development goals (SDGs).

Sixth, unfortunately, the polarization of agricultural intensification has increased in the last 25 years: some developed countries have explored sustainable intensification models relying on the advantages of fertile farmland, fine breeds and advanced agricultural technology; however, some other countries (mainly in Asia, America and Oceania) are limited by natural, scientific and economic factors and try to improve output intensity by increasing the input intensity of chemical fertilizer and pesticides. For most of them, these measures have had a poor effect on improving output intensity but have caused irreversible farmland ecosystem degradation, increased agricultural carbon emissions and loss of farmland biodiversity, and even threatened human health. Therefore, government actions to develop sustainable intensification need extensive international cooperation and support. Low SI countries need to promote international advanced agricultural technology and agricultural infrastructure and eliminate excessive dependence on chemical fertilizers and pesticides.

4.4. Develop input—output coupled analysis at multiple spatial-temporal scales

This study is a preliminary attempt to analyse the coupling effect of input intensity on output intensity at the province scale and thereby estimate the suitability of input intensity in China. The authors hold that the coupling—decoupling—recoupling process between input and output intensity can be regarded as the extension and application of Landau's theory of phase transition in the study of farmland ecosystem. According to Landau's theory of phase transition, the phase transition from gas to liquid is accompanied by a loss of symmetry, and the order parameter changes from zero to non-zero, indicating that the state of the system changes from disorder to order. Similarly, in the process of coupling to decoupling, the sliding window-based partial correlation coefficient changes from significant correlation (i.e., non-zero, $p < 0.05$) becomes irrelevant (i.e., zero), indicating that the promotion (or inhibition) effect of input intensity on output intensity has undergone a phase transition from order to disorder. The reversed phase transition occurs in the process of decoupling to re-coupling. The partial correlation coefficient, as the order parameter, effectively captures the phase transition process from a holistic perspective.

The limitation of this study is that the spatial heterogeneity of farming conditions (i.e., climatic conditions, soil properties, terrain features, and agricultural infrastructure conditions) has been ignored. Farming conditions influence the driving effect of input intensity on output intensity. For instance, Fig. 7(c-1) shows that the mulching film input intensity has the opposite effect on the output intensity of staple food grains in plain areas and mountain areas. To understand the influence of multi-element input intensity on output intensity, more input—output coupled analysis cases should be implemented in zones with homogeneous climatic conditions, soil properties, terrain features and agricultural infrastructure conditions (Gong et al., 2023; Jin et al., 2024; Ye et al., 2022c). Another important question is how farming conditions contribute to the input—output coupling process. Answering this question can provide support for exploring suitable arable land consolidation schemes. And the differences in the input–output coupling process caused by crop types should also be considered in follow-up studies. To achieve these objectives, abundant field-scale survey data or county-level agricultural statistical yearbook data related to agricultural input and output need to be collected, which puts forwards an urgent need for the imaging technology of satellite-ground fusion (Lu and Ye, 2020; Ye et al., 2014, 2020b; Wan et al., 2021) and high-performance spatial data processing and analysis techniques (Yao et al., 2017; Ye et al., 2016, 2018; Wang et al., 2022b). The input—output coupled analysis method is also applicable to higher scales, for instance, analysing the overall input–output coupling relationship at the global scale (Gao et al., 2023; Wang et al., 2023, 2024). Furthermore, this study mainly focuses on the estimation of sustainable intensification from the dimension of input-output relationship, and the sustainability of ecological function and social benefit dimension is not considered enough. Our future work will examine the effects of arable land use on farmland socio-ecosystem functions (Fang et al., 2022).

5. Conclusions

In this study, first, China's provincial annual input intensity and output intensity were estimated in the form of emergy. The results show that the output intensity of staple food grains (including rice; wheat; corn; beans; potato) and oil crops (oilseed and hemp) both showed a steady increase from 1998 to 2019, while most types of input intensity (i.e., fertilizer; pesticide; labour force; mulching film) experienced a process of first increasing and then decreasing. Provinces with the highest input intensity are clustered in the Huang-Huai-Hai Plain and Southern China with different combination structures, while Southern China does not show corresponding high output intensity. Second, the K-means algorithm was used to identify the structural pattern of the provincial annual arable land input intensity. The results show that there are two main change paths in the pattern of arable land input intensity: western regions mainly experienced a small increase in the input intensity of fertilizer and agro-machinery with a decrease in labour force input intensity, while the northeast China Plain, middle-lower Yangtze Plain and Central Shaanxi Plain experienced a larger increase in fertilizer and pesticide input intensity. Third, a sliding window-based partial correlation index method was proposed and applied to explain the impact of input intensity on output intensity and thereby estimate the suitability of provincial sustainable intensification (SI). The results show that for each type of input intensity, its correlation to output intensity has experienced a coupling—decoupling—recoupling process. These processes may show characteristics of opposition between mountainous regions and high-yield regions. The inflection point of coupling relation changes provides guidance for estimating the suitability of input intensity. According to these inflection points, the phenomenon of fertilizer and pesticide overuse has steadily occurred in most provinces in eastern China and is spreading westwards. The input intensity of fertilizer and pesticides needs to be further reduced. Forth, since 2015, China has embarked on a sustainable intensification route with decreasing fertilizer and pesticide input intensity and increasing output intensity. However, there is still an obvious gap between the output intensity of China and the world's leading level. Developing and disseminating land consolidation techniques and thereby improving arable land quality is of great significance for China to achieve the world's highest SI level. To understand the influence of multi-element input intensity on output intensity, more input—output coupled analysis cases should be implemented in zones with homogeneous climatic conditions, soil properties, terrain features and agricultural infrastructure conditions. The analysis method of this study can provide guidance for other countries to estimate the suitability of SI.

CRediT authorship contribution statement

Sijing Ye: Conceptualization, Formal analysis, Methodology, Visualization, Writing – original draft, Writing – review & editing. **Jilong Wang:** Data curation, Methodology, Resources, Visualization. **Jiayi Jiang:** Data curation, Methodology, Software, Visualization. **Peichao Gao:** Investigation, Methodology, Resources. **Changqing Song:** Conceptualization, Formal analysis, Funding acquisition, Project administration, Supervision.

Declaration of competing interest

The authors declare that they have no known competing financial interests or personal relationships that could have appeared to influence the work reported in this paper.

Data availability

I have shared the data

Acknowledgments

This research was funded by National Natural Science Foundation of China (Grant No. 42171250, 42230106); the second Tibetan Plateau Scientific Expedition and Research Program (STEP) (Grant No. 2019QZKK0608); and Project Supported by State Key Laboratory of Earth Surface Processes and Resource Ecology, China (2022-ZD-04). We would like to thank the high-performance computing support from the Center for Geodata and Analysis, Faculty of Geographical Science, Beijing Normal University (https://gda.bnu.edu.cn/).

Appendix A. Supplementary data

Supplementary data to this article can be found online at https://doi.org/10.1016/j.jclepro.2024.140827.

References

Brookfield, 1993. Brookfield H.C. Notes on the theory of land management. PLEC News and Views 1, 28–32.
Chen, X., Cui, Z., Vitousek, P., et al., 2011. Integrated soil–crop system management for food security. Proc. Natl. Acad. Sci. U.S.A. 108 (16), 6399–6404.
Cassman, K., Grassini, P., 2020. A global perspective on sustainable intensification research. Nat. Sustain. 3, 262–268.
Dietrich, J.P., Schmitz, C., Muller, C., et al., 2012. Measuring agricultural land-use intensity—a global analysis using a model-assisted approach. Ecol. Model. 232 (10), 109–118.
Desquilbet, M., Dorin, B., Couvet, D., 2017. Land sharing vs land sparing to conserve biodiversity: how agricultural markets make the difference. Environ. Model. Assess. 22 (3), 185–200, 2017.
Du, B., Ye, S., Gao, P., et al., 2024. Analyzing spatial patterns and driving factors of cropland change in China's National Protected Areas for sustainable management. Sci. Total Environ. 912, 169102.
Ewers, R., Scharlemann, J., Balmford, A., et al., 2009. Do increases in agricultural yield spare land for nature? Global Change Biol. 15 (7), 1716–1726.
Erb, K., 2012. How a socio-ecological metabolism approach can help to advance our understanding of changes in land-use intensity. Ecol. Econ. 76, 8–14.
Erb, K., Haberl, H., Jepsen, M., et al., 2013. A conceptual framework for analysing and measuring land-use intensity. Curr. Opin. Environ. Sustain. 5, 464–470.
Foley, J., DeFries, R., Asner, G., et al., 2005. Global consequences of land use. Science 309 (5734), 570–574.
Foley, J., Ramankutty, N., Brauman, K., et al., 2011. Solutions for a cultivated planet. Nature 478 (7369), 337–342.
Folberth, C., Khabarov, N., Balkovič, J., et al., 2020. The global cropland-sparing potential of high-yield farming. Nat. Sustain. 3, 281–289.
Fang, D., Cai, Q., Wu, F., et al., 2022. Modified linkage analysis for water-land nexus driven by interregional trade. J. Clean. Prod. 253, 131547.
Gao, P., Wang, Y., Wang, H., et al., 2023. A Pareto front-based approach for constructing composite index of sustainability without weights: a comparative study of implementations. Ecol. Indicat. 155, 110919.
Gregory, P.J., Ingram, J.S.I., Andersson, R., et al., 2002. Environmental consequences of alternative practices for intensifying crop production. Agric. Ecosyst. Environ. 88, 279–290.
Green, R., Cornell, S., Scharlemann, J., 2005. Farming and the fate of wild nature. Science 307 (5709), 550–555.
Garnett, T., Appleby, M., Balmford, A., et al., 2013. Sustainable intensification in agriculture: premises and policies. Science 341 (6141), 33–34.
Gong, B., Liu, Z., Liu, Y., et al., 2023. Understanding advances and challenges of urban water security and sustainability in China based on water footprint dynamics. Ecol. Indicat. 150, 110233.
Herzog, F., Steiner, B., Bailey, D., et al., 2006. Assessing the intensity of temperate European agriculture at the landscape scale. Eur. J. Agron. 24, 165–181.
Hertel, T., Ramankutty, N., Baldos, U., 2014. Global market integration increases likelihood that a future African Green Revolution could increase crop land use and CO2 emissions. Proc. Natl. Acad. Sci. U.S.A. 111 (38), 13799–13804.
Huang, Q., Zhang, H., van Vliet, J., et al., 2021. Patterns and distributions of urban expansion in global watersheds. Earth's Future 9 (8), e2021EF002062.
Jin, X., Jiang, W., Fang, D., et al., 2024. Evaluation and driving force analysis of the water-energy-carbon nexus in agricultural trade for RCEP countries. Appl. Energy 353, 122143.
Kuemmerle, T., Erb, K., Meyfroidt, P., et al., 2013. Challenges and opportunities in mapping land use intensity globally. Curr. Opin. Environ. Sustain. 5, 484–493.
Li, S., Fu, X., Zheng, D., 2001. Emergy analysis for evaluating sustainability of Chinese economy. J. Nat. Resour. 16 (4), 297–304 (in Chinese with English abstract).
Li, S., Lei, Y., Zhang, Y., et al., 2019. Rational trade-offs between yield increase and fertilizer inputs are essential for sustainable intensification: a case study in wheat–maize cropping systems in China. Sci. Total Environ. 679 (20), 328–336.
Lu, H., Chen, L., Lin, Y., et al., 2005. Emergy synthesis of the dynamics of the Shunde industrial system. Acta Ecol. Sin. 31 (9), 2188–2196 (in Chinese with English abstract).
Lal, R., 2019. Eco-intensification through soil carbon sequestration: harnessing ecosystem services and advancing sustainable development goals. J. Soil Water Conserv. 74 (3), 55a–61a.
Lu, S., Ye, S., 2020. Using an image segmentation and support vector machine method for identifying two locust species and instars. J. Integr. Agric. 19 (5), 1301–1313.
Liu, C., Song, C., Ye, S., 2023. Estimate provincial-level effectiveness of the arable land requisition-compensation balance policy in mainland China in the last 20 years. Land Use Pol. 131, 106733.
Malthus, T., 1798. An Essay on the Prinicple of Population. Printed for J. Johnson, in St. Paul's Church-Yard, London..
Mahon, N., Crute, I., Di Bonito, M., et al., 2018. Towards a broad-based and holistic framework of Sustainable Intensification indicators. Land Use Pol. 77, 576–597.
Mehrabi, Z., Ellis, E., Ramankutty, N., 2018. The challenge of feeding the world while conserving half the planet. Nat. Sustain. 1 (8), 409–412.
Mckay, D., Dearing, J., Dyke, J., et al., 2019. To what extent has sustainable intensification in England been achieved? Sci. Total Environ. 648 (15), 1560–1569.
Mouratiadou, I., Latka, C., Hilst, F., et al., 2021. Quantifying sustainable intensification of agriculture: the contribution of metrics and modelling. Ecol. Indicat. 129, 107870.
Neumann, K., Verburg, P.H., Stehfest, E., Muller, C., 2010. The yield gap of global grain production: a spatial analysis. Agric. Syst. 103, 316–326.
Pretty, J., Thompson, J., Hinchcliffe, F., 1996. Sustainable Agriculture: Impacts on Food Production and Food Security, vol. 60. International Institute for Environment and Development, Gatekeeper Series.
Pretty, J., 1997. The sustainable intensification of agriculture. Nat. Resour. Forum 21 (4), 247–256.
Pretty, J., Bharucha, Z., 2014. Sustainable intensification in agricultural systems. Ann. Bot. 8, 1571–1596.
Petersen, B., Snapp, S., 2015. What is sustainable intensification? Views from experts. Land Use Pol. 46, 1–10.
Phalan, B., Green, R., Dicks, L., et al., 2016. How can higher-yield farming help to spare nature? Science 351 (6272), 450–451.
Pretty, J., Benton, T., Bharucha, Z., et al., 2018. Global assessment of agricultural system redesign for sustainable intensification. Nat. Sustain. 1 (8), 441–446.
Ricardo, D., 1815. An Essay on the Influence of a Low Price of Corn on the Profits of Stock. John Murray, London.
Rosegrant, M., Cline, S., 2003. Global food security: challenges and policies. Science 302, 1917–1919.
Reich, J., Paul, S., Snapp, S., 2021. Highly variable performance of sustainable intensification on smallholder farms: a systematic review. Global Food Secur. 30, 100553.
Ren, S., Song, C., Ye, S., et al., 2022. The spatiotemporal variation in heavy metals in China's farmland soil over the past 20 years: a meta-analysis. Sci. Total Environ. 806, 150322.
Ren, S., Song, C., Ye, S., et al., 2023. Land use evaluation considering soil properties and agricultural infrastructure in black soil region. Land Degrad. Dev. 34 (17), 5373–5388.
Shriar, A., 2000. Agricultural intensity and its measurement in frontier regions. Agrofor. Syst. 49 (3), 301–318.
Smith, P., 2013. Delivering food security without increasing pressure on land. Global Food Secur. 2, 18–23.
Smith, A., Snapp, S., Chikowo, R., et al., 2017. Measuring sustainable intensification in smallholder agroecosystems: a review. Global Food Secur. 12, 127–138.
Tilman, D., Balzer, C., Hill, J., Befort, B.L., 2011. Global food demand and the sustainable intensification of agriculture. Proc. Natl. Acad. Sci. U.S.A. 108, 20260–20264.
Von Thuenen, J.H., 1826. Der isolierte Staat in Beziehung auf Landwirtschaft und Nationalokonomie oder Untersuchungen über den Einfluss, den die Getreidepreise, der Reichthum des Bodens und die Abgaben auf den Ackerbau ausüben. Friedrich Berthes, Hamburg.
Vanlauwe, B., Bationo, A., Chianu, J., et al., 2010. Integrated soil fertility management: operational definition and consequences for implementation and dissemination. Outlook Agric. 39 (1), 17–24.
Vanlauwe, B., Coyne, D., Gockowski, J., et al., 2014. Sustainable intensification and the African smallholder farmer. Curr. Opin. Environ. Sustain. 8, 15–22.
Wezel, A., Soboksa, G., Mcclelland, S., et al., 2015. The blurred boundaries of ecological, sustainable, and agroecological intensification: a review. Agron. Sustain. Dev. 35 (4), 1283–1295.
Wan, C., Kuzyakov, Y., Cheng, C., et al., 2021. A soil sampling design for arable land quality observation by using spcosa-clhs hybrid approach. Land Degrad. Dev. 32 (17), 4889–4906.
Wang, Z., Liu, X., Zhou, W., et al., 2022a. Land use intensification in a dry-hot valley reduced the constraints of water content on soil microbial diversity and multifunctionality but increased CO2 production. Sci. Total Environ. 852 (15), 158397.

Wang, K., Ye, S., Gao, P., et al., 2022b. Optimization of numerical methods for transforming utm plane coordinates to lambert plane coordinates. Remote Sens-Basel 14 (9), 2056.
Wang, Y., Song, C., Gao, Y., et al., 2024. Integrating national integrated assessment model and land-use intensity for estimating China's terrestrial ecosystem carbon storage. Appl. Geogr. 162, 103173.
Wang, Y., Song, C., Cheng, C., et al., 2023. Modelling and evaluating the economy-resource-ecological environment system of a third-polar city using system dynamics and ranked weights-based coupling coordination degree model. Cities 133, 104151.
Xie, H., Zou, J., Peng, X., 2012. Spatial-temporal difference analysis of cultivated land use intensity based on emergy in Poyang Lake Eco-economic Zone. Acta Geograph. Sin. 67 (7), 889–902 (in Chinese with English abstract).
Xie, H., Huang, Y., Choi, Y., Shi, J., 2020. Evaluating the sustainable intensification of cultivated land use based on emergy analysis. Technol. Forecast. Soc. Change 165 (1), 120449.
Yao, G., Liu, G., Xie, H., 2014a. Spatiotemporal difference and driving forces of input factors intensity for arable land-use in China. J. Nat. Resour. 29 (11), 1836–1848 (in Chinese with English abstract).
Yao, C., Huang, L., Lv, X., 2014b. Temporal and spatial change of cultivated land use intensity in China based on emergy theory. Trans. Chin. Soc. Agric. Eng. (8), 1–12 (in Chinese with English abstract).
Yao, X., Mokbel, M., Ye, S., et al., 2017. Spatial coding-based approach for partitioning big spatial data in Hadoop. Comput. Geosci. 106, 60–67.
Ye, S., Zhu, D., Yao, X., et al., 2014. Development of a highly flexible mobile GIS-based system for collecting arable land quality data. IEEE J-Stars. 7, 4432–4441.
Ye, S., Yan, T., Yue, Y., et al., 2016. Developing a reversible rapid coordinate transformation model for the cylindrical projection. Comput. Geosci.-Uk 89, 44–56.
Ye, S., Liu, D., Yao, X., Tang, H., et al., 2018. RDCRMG: a raster dataset clean & reconstitution multi-grid architecture for remote sensing monitoring of vegetation dryness. Rem. Sens. 10 (9), 1376.
Ye, S., Song, C., Cheng, F., et al., 2019. Cultivated land health-productivity comprehensive evaluation and its pilot evaluation in China. Trans. Chin. Soc. Agric. Eng. 35 (22), 66–78 (in Chinese with English abstract).
Ye, S., Song, C., Shen, S., et al., 2020a. Spatial pattern of arable land-use intensity in China. Land Use Pol. 99, 104845.
Ye, S., Lu, S., Bai, X., et al., 2020b. ResNet-locust-BN network-based automatic identification of east asian migratory locust species and instars from RGB images. Insects 11 (8), 458.
Ye, S., Ren, S., Song, C., et al., 2024. Spatial pattern of cultivated land fragmentation in mainland China: characteristics, dominant factors, and countermeasures. Land Use Pol. 139, 107070.
Ye, S., Ren, S., Song, C., Cheng, C., et al., 2022a. Spatial patterns of county-level arable land productive-capacity and its coordination with land-use intensity in mainland China. Agric. Ecosyst. Environ. 326, 107757.
Ye, S., Song, C., Gao, P., Liu, C., Cheng, C., 2022b. Visualizing clustering characteristics of multidimensional arable land quality indexes at the county level in mainland China. Environ. Plann.: Econ. Space 54 (2), 222–225.
Ye, S., Song, C., Kuzyakov, Y., et al., 2022c. Preface: arable land quality: observation, estimation, optimization, and application. Land 11 (6), 1–5.
Ye, S., Song, C., Gao, P., et al., 2023. Construction of the new cognitive system for arable land resources from geospatial perspective. Transac. CSAE 39 (9), 225–240.
Yin, G., Lin, Z., Jiang, X., et al., 2018. Spatiotemporal differentiations of arable land use intensity — a comparative study of two typical grain producing regions in northern and southern China. J. Clean. Prod. 208, 1159–1170.
Yin, G., Jiang, X., Sun, J., Qiu, M., 2020. Discussing the regional-scale arable land use intensity and environmental risk triggered by the micro-scale rural households' differentiation based on step-by-step evaluation—a case study of Shandong Province, China. Environ. Sci. Pollut. Control Ser. 27 (8), 8271–8284.
Yin, D., Huang, Q., He, C., et al., 2022. The varying roles of ecosystem services in poverty alleviation among rural households in urbanizing watersheds. Landsc. Ecol. 37 (6), 1673–1692.
Zhang, X., Davidson, E., Mauzerall, D., et al., 2015. Managing nitrogen for sustainable development. Nature 528 (7580), 51–59.
Zhang, X., Bol, R., Rahn, C., et al., 2017. Agricultural sustainable intensification improved nitrogen use efficiency and maintained high crop yield during 1980–2014 in Northern China. Sci. Total Environ. 596–597 (15), 61–68.
Zingg, S., Grenz, J., Humbert, J., 2018. Landscape-scale effects of land use intensity on birds and butterflies. Agric. Ecosyst. Environ. 267, 119–128.